Title

Influence of the Coast and Vegetation on Temperature Gradients across the Los Angeles Basin using Mobile Transect Techniques

Permalink

https://escholarship.org/uc/item/3g13r235

Author

Lee, Audrey

Publication Date

2012

Peer reviewed|Thesis/dissertation

UNIVERSITY OF CALIFORNIA

Los Angeles

Influence of the Coast and Vegetation on Temperature Gradients across the Los Angeles

Basin using Mobile Transect Techniques

A thesis submitted in partial satisfaction

of the requirements for the degree Master of Science

in Civil Engineering

by

Audrey Michelle Lee

2012

ABSTRACT OF THE THESIS

Influence of the Coast and Vegetation on Temperature Gradients across the Los Angeles

Basin using Mobile Transect Techniques

by

Audrey Michelle Lee

Master of Science in Civil Engineering

University of California, Los Angeles, 2012

Professor Steven A. Margulis, Co-Chair

Professor Terri S. Hogue, Co-Chair

Temperature rise, caused by urbanization, increases electricity demand, adversely affects human

health, and alters hydrological and ecological patterns. Urban heat islands (UHI) are affected by

both complex urban cover as well as surrounding environments. This study describes the

variability of temperature and relative humidity as it is (1) influenced by local vegetation and

land cover type over neighborhoods and (2) moderated by coastal climate across the urban

gradient. Data were collected at four different times of the day during three different weather

conditions using mobile transects over four urban neighborhoods in Southern California: Venice,

Mid-Wilshire, Pomona, and Riverside. The four neighborhoods also form a climate gradient

extending from the Venice (coast) to Riverside (99 miles inland). The influence of urban land

cover on local climate proved dependent on the time of day and general atmospheric conditions (sunny, cloudy, etc). Temperature was statistically related to vegetation during cooler or early morning measurements, but less so during midday and extreme heat conditions. Inland neighborhood temperatures and relative humidity showed an increased dependence on vegetation from coastal areas because of the lack of other moisture sources. This study serves as an initial baseline for continued study of the urbanization of coastal and inland areas and relationship to local land cover and vegetation density.

The thesis of Audrey Michelle Lee is approved.

Darrel Jenerette

William W-G. Yeh

Steven A. Margulis, Committee Co-Chair

Terri S. Hogue, Committee Co-Chair

University of California, Los Angeles

2012

Acknowledgements

I would like to thank Terri Hogue for her guidance and leadership on this research as well as her patience and confidence in me. I would also like to thank Jongyoun Kim and Brandon Hale for their help in utilizing data analysis programs and encouraging me throughout this process. Thanks to Forest and his team for aiding in data collection. A special thank you to Steve Margulis whose classes first interested me in research and whose encouragements and advice led me to graduate studies. A loving thank you to all my roommates, friends, and family who endured my late night work, humored me with discussions about data and research, and prayed for me during hardship. I thank Jesus Christ, my Lord and savior, for the amazing opportunities that He has blessed me with and the strength that He has given me during this process. Lastly, I would like to thank my committee, Terri Hogue, Steve Margulis, Darrel Jenerette, and William Yeh, for their input and time in helping me through this adventure.

Table of Contents

List of Figures

Appendix Figures

List of Tables

Appendix Tables

Introduction

After the first observation of the urban heat island (UHI) effect in London, England by Luke Howard, multiple studies have undertaken to determine the degree of influence of urbanization on earth processes (Zhang et al., 2008). Measurements have been made to determine the temperature differences between recently urbanized areas and their surrounding rural areas. Compared to known global warming effects from greenhouse gases, the UHI phenomenon has been proven to be more rapid. In the last century, the urbanized cities of Japan have been shown to increase in temperature by approximately $3^{o}C$ while the mean global temperature has increased by a mere 0.3-$0.6^{o}C$ (Zhang, et al. 2008).

Studies such as one made in Łódź, Poland by Fortuniak et al. (2006) have shown that increases in temperature and urbanization caused changes in the area's relative humidity, water vapor pressure, and wind speeds. The altering of natural occurring patterns has caught the attention of many scientists because of the dangerous and costly implications of these changes to the surrounding atmosphere, hydrologic cycle, and human health. UHI effects have shown to escalate local threats of heat waves, increase energy demand for air conditioning, degrade air quality, adversely affect urban climate, and influence vegetation and bio diversity (Zhang, et al. 2008; Houet and Pigeon, 2011).

UHIs are developed through a combination of the many changes caused by urban expansion. Aside from direct anthropomorphic heat emissions, two prominent causes of UHI are changes in land cover and a city's geometric and physical structure. The impact of an UHI on an area's climate can change depending on the natural or background climate of an area and the specifics of the city design. Materials in urban areas have very different physical and chemical characteristics than the original land cover. The reduction of vegetation and free water surfaces

can greatly impact the heat over an area. This is largely due to the decrease in radiation energy partitioning to the latent heat flux. In a previous study over Los Angeles, California, 19% more energy was measured over an area with 30% tree and shrub cover than a nearby neighborhood with 10% vegetation cover (Arnfield, 2003). Heat increases are also attributed to the overall decrease in perviousness of materials used for buildings and roads. Bare soil temperatures tend to be lower than covered surfaces because of the hydrological behavior of the materials. Bare soil typically allows for infiltration and the holding of water. The mixing and matching of different types of buildings, roads, and vegetation can also affect the amount of heat that is dispersed into the air. Houet and Pigeon (2011) studied the effect of different variations of building and vegetation height and density on the thermal fluxes in urban canyons. The effects of urban canyon geometry and material properties have in some cases shown to be of almost equal significance to effects of direct thermal point emissions (Arnfield, 2003).

Temperature increase over urban areas is also affected by surrounding climate patterns and geography. Because sources of water play a key role in the energy balance, the UHI over coastal areas created by loss of vegetation is mitigated. Lin et al. (2011) modeled the urban canopy over an area of Taipei, Taiwan. The study showed changes in the precipitation placement and rates over the city based on the UHI as well as the impacts of the coast and mountain region. The UHI both contributed to and was affected by the land-sea circulation patterns and airflow by the mountainous barrier.

Seasonality also plays a key role in the intensity of an observed UHI. The largest differences between rural and urban temperatures occur during night and winter seasons (Fortuniak et al., 2006). This is due in part to the increase in anthropomorphic heat from electricity and gas use in buildings for internal heating. However, the partitioning of latent heat

causes UHI intensities to be typically higher during dry seasons versus wet seasons because of the availability of water sources (Arnfield, 2003). Studies over dry areas have shown heat storage in urban areas of up to 58%; meaning that heat be trapped within the fabric of the city during the night while nearby rural areas would cool (Arnfield, 2003). The angles and intensities at which building walls and streets intercept both short and long wave radiation would vary with the positioning of the earth with respect to the sun (Zhang et al., 2008). Many UHI studies are particularly interested in the summer months because of the increased temperature and amount of extreme heat days. Extreme heat causes increased electricity demand and deficits during the summer months from the use of air conditioning as well as causing adverse effects in human health (Miller et al., 2007). A study by Miller et al. (2007) showed the number of extreme heat days could increase two to four times the present-day number for coastal and inland California cities.

The expansion of urban areas worldwide has led to the development of several methodologies for studying the multiple aspects of UHI. Major methods of measurement have involved utilizing fixed weather stations, satellite imagery, vertical soundings launched through the atmosphere, and mobile transects depending on the specific variables of study (Arnfield, 2003). Mobile transects allow for measurements at a larger spatial scale than fixed ground stations and are unaffected by cloud cover that can disrupt satellite imagery. Mobile measurements have the ability to traverse through areas that have little historical climatological information or sparsely spaced weather stations (Hedquist et al., 2006). Mobile measurements also collect data over multiple land cover types. Through mobile measuring devices, specific areas of interest can be chosen for study and comparison. With this method, changing land cover

types can be connected to climate variables through detailed measurements over a large spatial scale that is economically and physically impractical through the use of stationary devices.

The current study utilizes measurements of temperature and relative humidity collected by mobile transects to describe the variability of temperature and relative humidity as it is: (1) influenced by local vegetation and land cover type over a diverse set of neighborhoods and (2) moderated by the coastal climate across the urban gradient. Mobile met data were collected over four neighborhoods in Southern California: Venice, Mid-Wilshire, Pomona, and Riverside. The influence of local vegetation and land cover type in the studied urban areas is evaluated at the neighborhood scale using data collected by the National Aeronautics and Space Administration (NASA) satellite Landsat 5 and data from the 2001 National Land Cover Database (NLCD). Influence of the coast on UHI is seen through connecting the geographical placement of the neighborhoods and the measured climate variables. Mobile measurements are also compared to regional ground based data from the National Climatic Data Center (NCDC) (administered by National Oceanic and Atmospheric Administration (NOAA)) and the California Irrigation Management Information System (CIMIS) run by the Department of Water Resources Office of Water use Efficiency in California.

Background

The method of measuring urban heat island (UHI) effects and variability through the use of mobile transects began as early as the 1970s and has been increasing in the last several years. In Phoenix, Arizona, Brazel and Johnson (1980) began a continuous study of UHI using a car and reanalysis of the same transect over the course of several years (Balling and Brazel, 1987; Hedquist and Brazel, 2006). The series of studies have each focused on different aspects of UHI in an arid region. Through their studies they have seen climate change with respect to rapid land

4

cover changes, and have made synoptic climatological links to UHI frequency and magnitude at a fine spatial scale that has been used as inputs for mesoscale models over Phoenix. In the UK, a series of UHI studies are being made using bicycles to sample air temperature over small towns where it would be economically and physically infeasible to secure established climate measurement sites (Melhuish and Pedder, 1998; Brandsma and Wolters, 2012). These studies have allowed for micro scale sampling of temperature change through neighborhood areas and have yielded important insights into the causes of UHI. While coastal influence has been shown in the past, there are still limited UHI studies over coastal areas, especially in Mediterranean regions. Over Los Angeles, there are a sparse amount of fixed climate stations, most of which are located in airports or have significant lapses in data. Using the mobile transect method, UHI can be tracked at a micro scale level with varying land cover types.

Because of the prominent influence of the coast on the Los Angeles region, several studies have described the marine air penetration into the inland areas at large spatial scales. Several studies concluded that the temperature changes in the coastal waters caused thermal upwelling, increased relative humidity, and cloud cover which not only affected coastal areas but also the temperature gradients farther inland (Dorman and Koračin, 2008; Bakun, 1990). A study by Lebassi et al. (2011) over a 35 year period used several coastal weather stations by the California National Weather Service Cooperative Observer Program and simulations of sea breeze patterns to model the large scale impacts of coastal flows. The study showed that sea breeze patterns played a part in the increase of temperature inland reaching the western edge of Riverside County. The study also demonstrated a history of asymmetrical increase in temperature with minimum temperatures increasing faster than maximum temperatures. However, each of these studies covered the Los Angeles County to Riverside County

temperatures at coarse domains. Grimmond et al., (1996; 1998) investigated UHI effects in areas including the San Gabriel Valley. These studies showed slight temperature increases in areas that were less urbanized and with more vegetation.

Study Areas

The four study neighborhoods are located in Southern California stretching over Los Angeles and Riverside County (figure 1). The neighborhoods chosen for each transect are representative of the growing urban landscape across the region and also form a coastal to inland gradient. The general physical characteristics of each neighborhood are summarized in table 1. Percentages of the land cover types and vegetation that were sampled over for each neighborhood are shown in table 2. According to the 2000 Census, the Mid-Wilshire area is the most populated of the four neighborhoods, while Riverside is the least populated. In terms of urban land cover, the coastal regions are the most urbanized with growing percentages of open space farther inland. For the purposes of this study, Venice is designated as the "coastal" neighborhood.
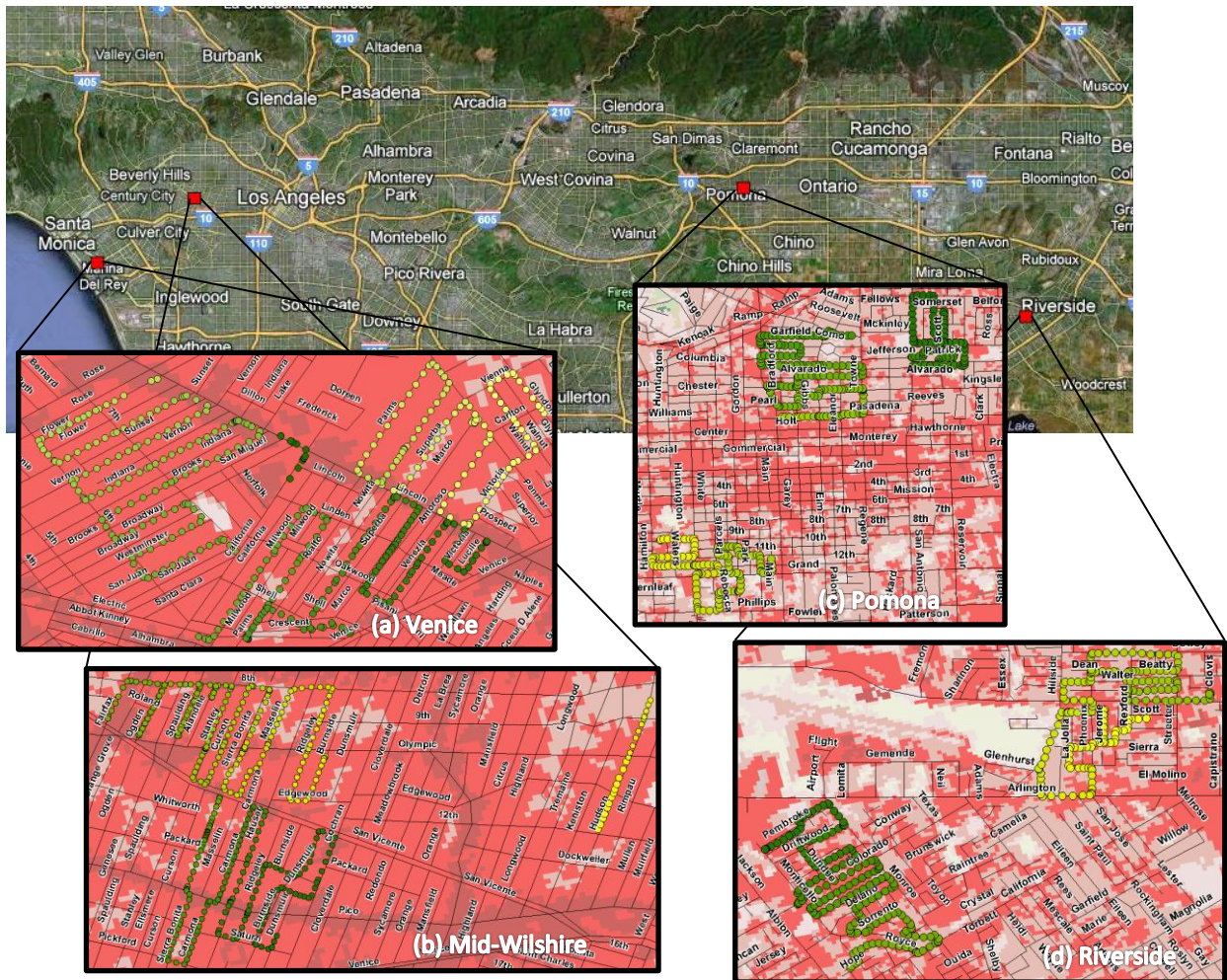
Figure 1 Study area map denoting land cover and path of travel from yellow to green

Table 1 Study area characteristics

Area	Latitude/ Longitude Centers	Area (km^2)	Distance from coast (km)*	Elevation above sea level (m)	Population/ km^2
Venice	33°59'46.53"N 118°27'40.16"W	2.07	-	5	4,591
Mid-Wilshire	34° 3'10.16"N 118°21'11.37"W	4.70	11.78	70	5,787
Pomona	34° 3'44.08"N 117°44'50.50"W	10.28	66.32	259	2,506
Riverside	33°56'45.39"N 117°26'1.01"W	8.36	95.12	262	1,467

* Coastal distances calculated through the latitude and longitude centers of each neighborhood with Venice designated as coast (0 km)

Table 2 Neighborhood land cover and NDVI

Neighborhood	Land Cover		NDVI			
	Index*	% Total	Mean	Max	Min	Variance
Venice	2	21.75	0.2494	0.5135	0.0299	0.0079
	3	70.83				
	4	7.42				
Mid-Wilshire	2	20.82	0.2600	0.6842	0	0.0173
	3	64.08				
	4	15.10				
Pomona	2	5.13	0.2538	0.5202	0.0426	0.0077
	3	52.12				
	4	30.63				
	5	10.11				
	8	0.75				
	11	1.27				
Riverside	2	5.48	0.2961	0.5645	0.0454	0.0046
	3	40.12				
	4	42.15				
	5	1.53				
	15	10.72				

* Refer to table [ ] for land cover index equivalents

The summer climate of California is subjected to the Pacific High as well as the coastal current system. These cause wind stresses alongshore that result in upwelling of cold water to the coastal surface (Lebassi et al., 2011; Bakun, 1990). The current system creates an elevated inversion layer that caps the marine boundary layer. The strong pressure, temperature, and moisture gradients off the coast can penetrate far inland in the Southern California coast. The coastal plain is open to the ocean with mountain ranges, northward of San Gabriel and San Bernardino and southeastward of Lakeview and Estelle Mountains, directing flows inland to the east.

Methods

Frequency and Dates of Measurement

Measurements were taken over three different repetitions for each of the four study

neighborhoods during four specific times of the day: 4am, 10am, 2pm, and 10pm (which will be

referred to in military time as hour 4, 10, 14, and 22). The three repetitions were taken during

mild (Rep1), heat wave (Rep2), and overcast (Rep 3) weather conditions to capture the extent of

coastal influence and its dependence on regional climate conditions. The weather conditions

were categorized based on observation and historical station data. Heat wave days, or extreme

heat days, for Rep 2 were defined having minimum and maximum temperatures above the

threshold for the 90th- percentile exceedence probability (T90) of the local maximum summer

temperatures during 2010 (June to September). Table 3 shows a summary of temperatures

measured at the NCDC USC station. This station is commonly used to represent the Los Angeles

Metropolitan area. The temperatures for the long term measurements of August and September

are averages taken from 2000-2010. Days used for Rep 3 were physically observed to be

overcast with grey cloudy skies. For each time of day and repetition, the same transects were

traveled over each neighborhood (figure 1) with yellow representing the start of measurements

and green the end of the measurement cycle. A summary of the data collection dates and times

are listed in table 4.

Table 3 Downtown Los Angeles (USC) Station Temperature Averages

Rep/Month	Average Temp (^{o}C)	Mean Max Temp (^{o}C)	Mean Min Temp (^{o}C)
1	20.08	25.43	16.79
2	25.46	31.25	21.40
3	20.46	24.17	17.63
Aug	23.31	28.52	18.07
Sept	22.74	28.13	17.33
T90	NA	30.00	18.30

The measured data were trimmed in order to match the measurement times of each location and repetition. The data for Venice Rep 2 was not used in the trimming of the time extents of the data because the beginning of the collection time began at approximately 11am, much later than all other data collected. After matching the repetition times, the beginning 15 minutes and last 4 minutes of each set were removed to allow for spin up and dismantling of the instruments. Finally, data outside of three standard deviations from the mean (less than 0.5% of the data) were removed. Location data were recorded through a separate GPS device which simultaneously recorded latitude and longitude. Temperature and relative humidity measurements were matched with location based on the time of measurements. GPS location recorded times did not always exactly match the times recorded with the probe; in these instances the location taken within five seconds of the probe's measured time was used.

Table 4 Data Collection Summary

Location	Date (DOY)	Weather	Landsat Pass used for NDVI
Venice	8/13/2010 (225)	Mild	8/9/2010
	8/25/2010 (237)	Heat Wave	8/25/2010
	9/8(9)/2010 (251/252)*	Overcast	9/10/2010
Mid-Wilshire	8/12/2010 (224)	Mild	8/9/2010
	8/24/2010 (236)	Heat Wave	8/25/2010
	9/7(8)/2010 (250/251)*	Overcast	9/10/2010
Pomona	8/11/2010 (223)	Mild	8/18/2010
	8/27(28)/2010 (239/240)**	Heat Wave	8/18/2010
	9/10(11)/2010 (253/254)*	Overcast	9/3/2010
Riverside	8/10/2010 (222)	Mild	8/18/2010
	8/26/2010 (238)	Heat Wave	8/18/2010
	9/9(10)/2010 (252/253)*	Overcast	9/3/2010

*4am measurements taken the day after other repetition measurements
** 10pm measurements taken the day after other repetition measurements

Instrumentation and Equipment

A car fitted with a temperature and relative humidity (RH) probe made by Campbell Scientific was used for mobile measurements. The probe utilized was the HMP45C with a HUMICAP® capacitive polymer H-chip to measure RH and a Platinum Resistance Thermometer (PRT) to measure temperature. The sensor has a diameter of 1in, a length of 10in and a response time of 15s. The RH can be measured within a range of 0.8-100% with accuracy of ±2% (0-90% RH) and ±3% (90-100% RH). The PRT has a measurement range of -39.2°C to +60°C. For the range of temperatures measured in this study, the PRT has an accuracy of ±0.3°C. The probe was mounted outside the vehicle in the front and center of the roof. This location was chosen so that measurements would not be biased by the car engine. Refer to figure 2 for a photo of the mounting of the instrumentation.

Figure 2 Equipment and instrumentation set-up

Land cover and Vegetation Data

Vegetation biomass was estimated using the normalized difference vegetation index (NDVI) calculated through Landsat 5 data at a 30m spatial level. A summary of the Landsat pass dates used for the collection of NDVI is shown in table 4.

Land cover/land use was estimated using the 2001 National Oceanic and Atmospheric Administration (NOAA) Coastal Change Analysis Program (C-CAP) that was revised to match the National Land Cover Database (NLCD). It is comprised of a 16-class land cover classification scheme (of which 7 are found in the areas of study) with a resolution of 30m. A description of the classification and indices used in this study are shown in table 5. Classifications were found using a combination of Landsat data and aerial photography through classification algorithms described by Vogelmann et al. (1998). In order to match the data with

the coarser spatial scale of vegetation and land use data, the location data of probe measurements were matched to the closest latitude and longitude available on the Landsat and NLCD maps.

Table 5 Pertinent C-CAP land cover classifications

Index	Classification	Description
2	Developed, High Intensity	Significant land area covered by concrete, asphalt, and other constructed materials. Vegetation, if present, occupies < 20 percent of the landscape. Constructed materials account for 80 to 100 percent of the total cover. This class includes heavily built-up urban centers and large constructed surfaces in suburban and rural areas with a variety of land uses.
3	Developed, Medium Intensity	Mixture of constructed materials and vegetation or other cover. Constructed materials account for 50 to 79 percent of total area. This class commonly includes multi- and single-family housing areas, especially in suburban neighborhoods, but may include all types of land use.
4	Developed, Low Intensity	Mixture of constructed materials and substantial amounts of vegetation or other cover. Constructed materials account for 21 to 49 percent of total area. This class commonly includes single-family housing areas, especially in rural neighborhoods, but may include all types of land use.
5	Developed, Open Space	Mixture of some constructed materials, but mostly managed grasses or low-lying vegetation planted in developed areas for recreation, erosion control, or aesthetic purposes. Constructed surfaces account for less than 20 percent of total land cover. These areas are maintained by human activity such as fertilization and irrigation. Features such as golf courses, cemeteries, and parks are included in this land use type.
8	Grassland/ Herbaceous	Dominated by grassland or herbaceous vegetation, generally greater than 80 percent of total vegetation. These areas are not subject to intensive management such as tilling, but can be utilized for grazing.
11	Mixed Forest	Dominated by trees generally greater than 5 meters tall, and greater than 20 percent of total vegetation cover. Neither deciduous nor evergreen species are greater than 75 percent of total tree cover. Both coniferous and broad-leaved evergreens are included in this category.
15	Palustrine Emergent Wetland	Tidal and nontidal wetlands dominated by persistent emergent vascular plants, emergent mosses or lichens, and all such wetlands that occur in tidal areas in which salinity due to ocean-derived salts is below 0.5 percent. Total vegetation cover is greater than 80 percent. Plants generally remain standing until the next growing season.

Results and Discussion

Data Variability

      Data collected during each run had slight variances in every neighborhood. These variances are due to land cover changes over each transect, the slight time change during measurements, and other physical surrounding factors. Figure 3 shows the spread of data for Rep 3 as a representative example of the variation of data for each run. Temperatures during runs were typically had a range of 1°C while relative humidity could vary up to 10% depending on the circumstance.
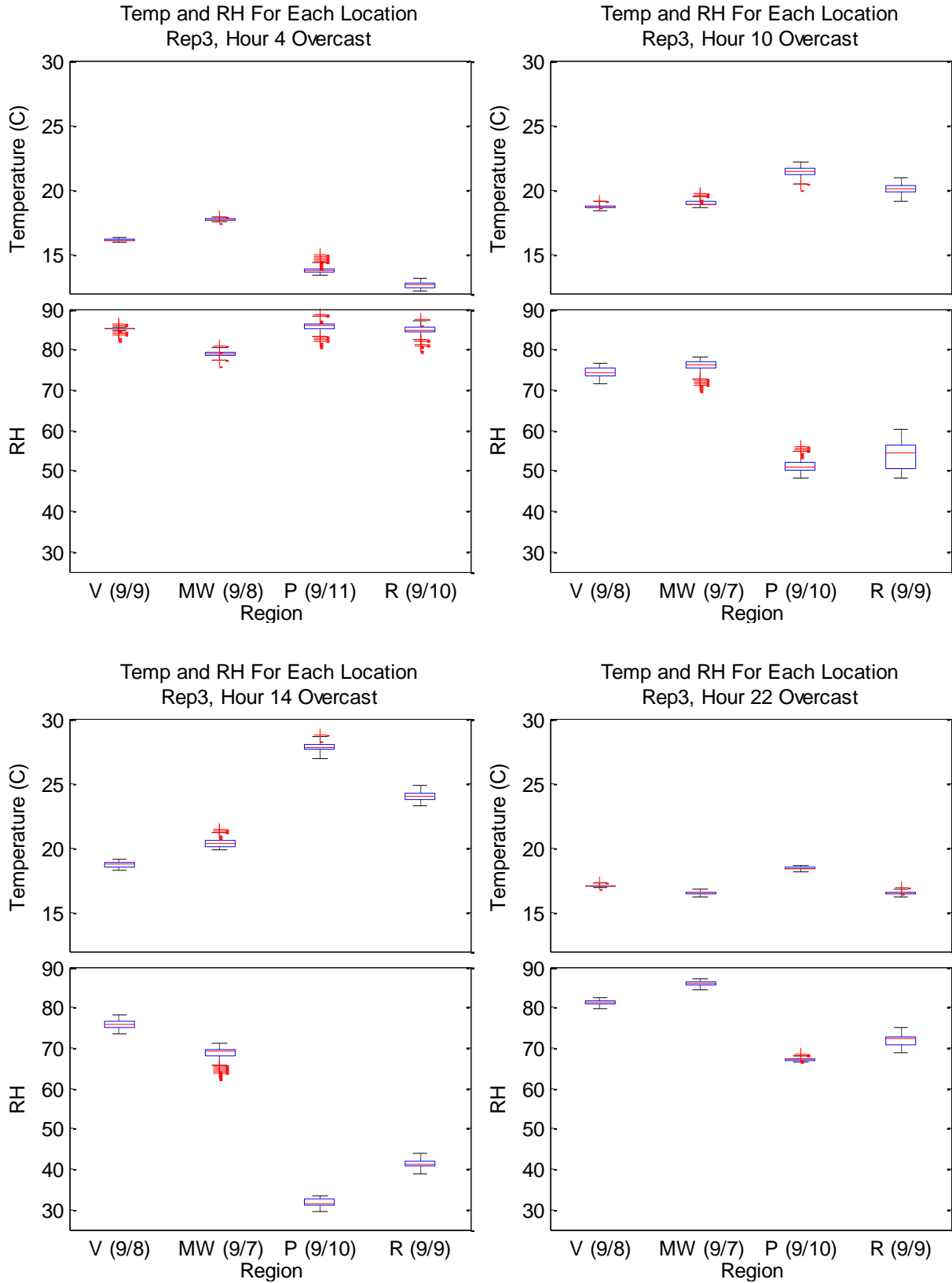
Figure 3 Temperature and RH Box Plots Rep 3

Temperature and Relative Humidity Comparison over Varying Weather Conditions

      The data shown for Rep 1 are an indication of the temperature and relative humidity (RH) trends on an average day. As expected, there are gradients of increasing and decreasing temperature throughout the day with the highest temperatures at hour 14 in each location. Temperatures are warmer midday with decreasing temperature observed for neighborhood locations near the coast (figure 4). However, the inverse is observed during hour 4 where the temperature is warmer near the coast than inland. The difference in the rate of change of temperature for each location over the course of the day shows the influence of the ocean on the moderation of temperature fluctuation.

      An inverse relationship can be seen in the plot of RH. Unfortunately the data collected during the 10am run in Riverside contained many erroneous points which could have been caused by passing cars, or problems with the probe. However, the average or expected temperature during that time in Riverside can be assumed by the trends of the other locations. It is interesting to note the relationship between Mid-Wilshire and Pomona during the 10am run. From 4am to 10am, the temperature and RH between these two locations is extremely similar, but divert as they approach 2pm with the temperature in Pomona increasing at a much higher rate.
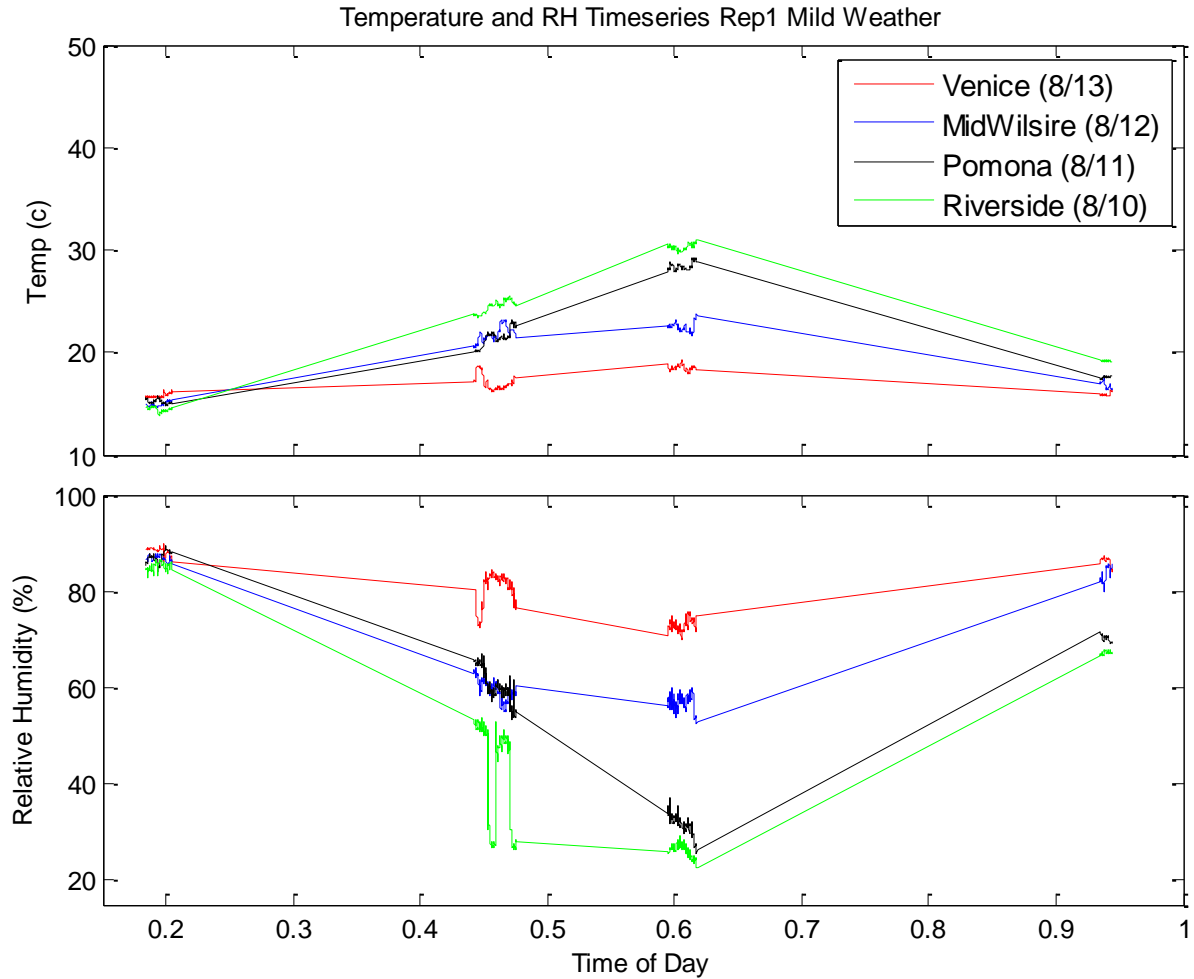
Figure 4 Comparison of the temperature and relative humidity (RH) for each run for Rep 1 over all measured locations during mild weather.

The trends of temperature and RH during Rep 2 (heat wave) are similar to those of Rep 1 (mild weather), but the differences are more pronounced. Once again the temperatures and RH over Pomona and Mid-Wilshire are very similar especially during the 10am run. However, the RH over Riverside has a slightly different trend than what is expected. There is a large drop in RH from morning to midday, but the RH over Riverside is the only location at which the RH does not recover at the end of the day, remaining relatively dry past 10am. This is particularly interesting because Riverside averages higher amounts of vegetation and least urban land cover

compared to the three other neighborhoods. Typically, RH is correlated with vegetation because of an areas' ability to store water (Stabler et al., 2005). In this case, the low RH in the evening hours is likely due to the distance from the ocean or other moderating bodies of water. The ocean is a large atmospheric moisture source for coastal cities. The evaporation over the water in combination with winds moving inland replenish moisture over the neighborhoods, but may not flow far enough inland to reach the Riverside location. Therefore, the coastal influence during the heat wave appears to have been significantly reduced within the 29 km distance between the locations of Pomona and Riverside.
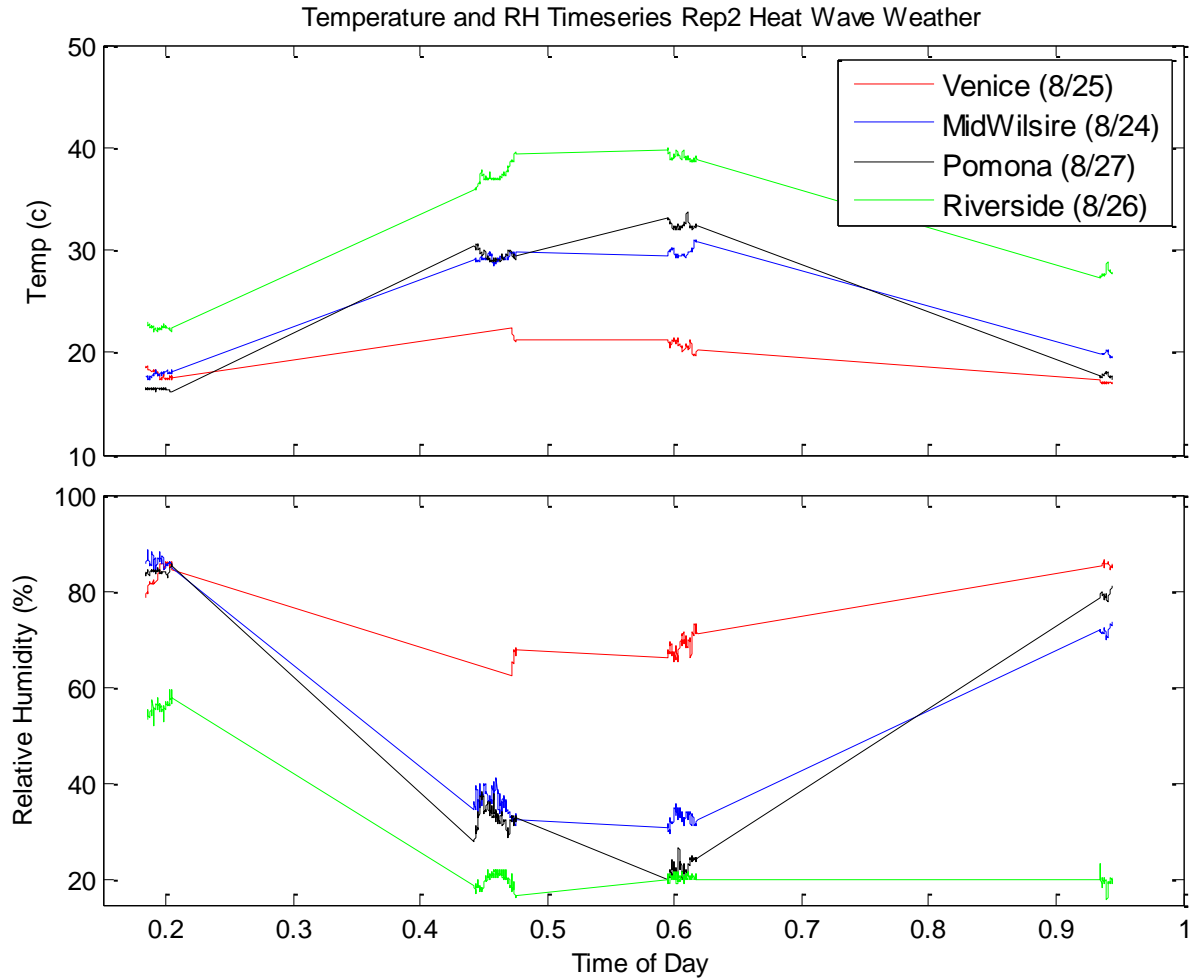
Figure 5 Comparison of the temperature and relative humidity (RH) for each run for Rep 2 over all measured locations during a heat wave.

During overcast weather, the temperature and relative humidity (RH) show a distinct separation between the cities closer to the coast and the cities that are inland. While each location shows the greatest temperatures and lowest RH midday, the change in temperature and RH is more gradual over Mid-Wilshire and Venice than they are over Pomona and Riverside. The early morning temperatures over the inland locations begin lower than the coastal locations but quickly become warmer than the inland locations by hour 14. This once again shows the effects of the ocean on moderating temperature over the study areas.

Interestingly, the pattern seen in the matching temperatures between Mid-Wilshire and Pomona do not occur during overcast weather conditions. In the previous repetitions, the temperature over Mid-Wilshire and Venice were almost equivalent at hour 10 and diverged by hour 14. In this case, the temperatures at hour 10 are already distinct between Mid-Wilshire and Pomona. The diversion of the temperatures over the two neighborhoods are seen during Rep 1 and 2 where morning temperatures over Mid-Wilshire and Pomona increased at similar rates until midday, at which Mid-Wilshire temperatures continued to rise while Mid-Wilshire temperatures began to cap, rising at a much slower rate. This may be due to the influence of the coastal air flows and the moisture gradients from the ocean whose cooling effects mediate temperature rise during midday. In the case of overcast weather, the temperature gradient over Mid-Wilshire is already controlled by high moisture levels and cloud cover so that even the initial heating in the morning does not occur, causing the diversion of temperatures between Mid-Wilshire and Pomona to occur earlier in the day.

It is important to note that the variance in temperatures between stations may be slightly skewed because of the different sampling days. While measurement days were consecutive, the weather conditions vary from day to day, which could cause a slight discrepancy when comparing the measurements for two sites. In the case of the measurements during Overcast weather, the temperatures over Pomona are shown to be higher than those of Riverside. Use of station data confirms that this is because of the difference in overall temperatures between September 9th and 10th as these dates are near the conclusion of the overcast period.
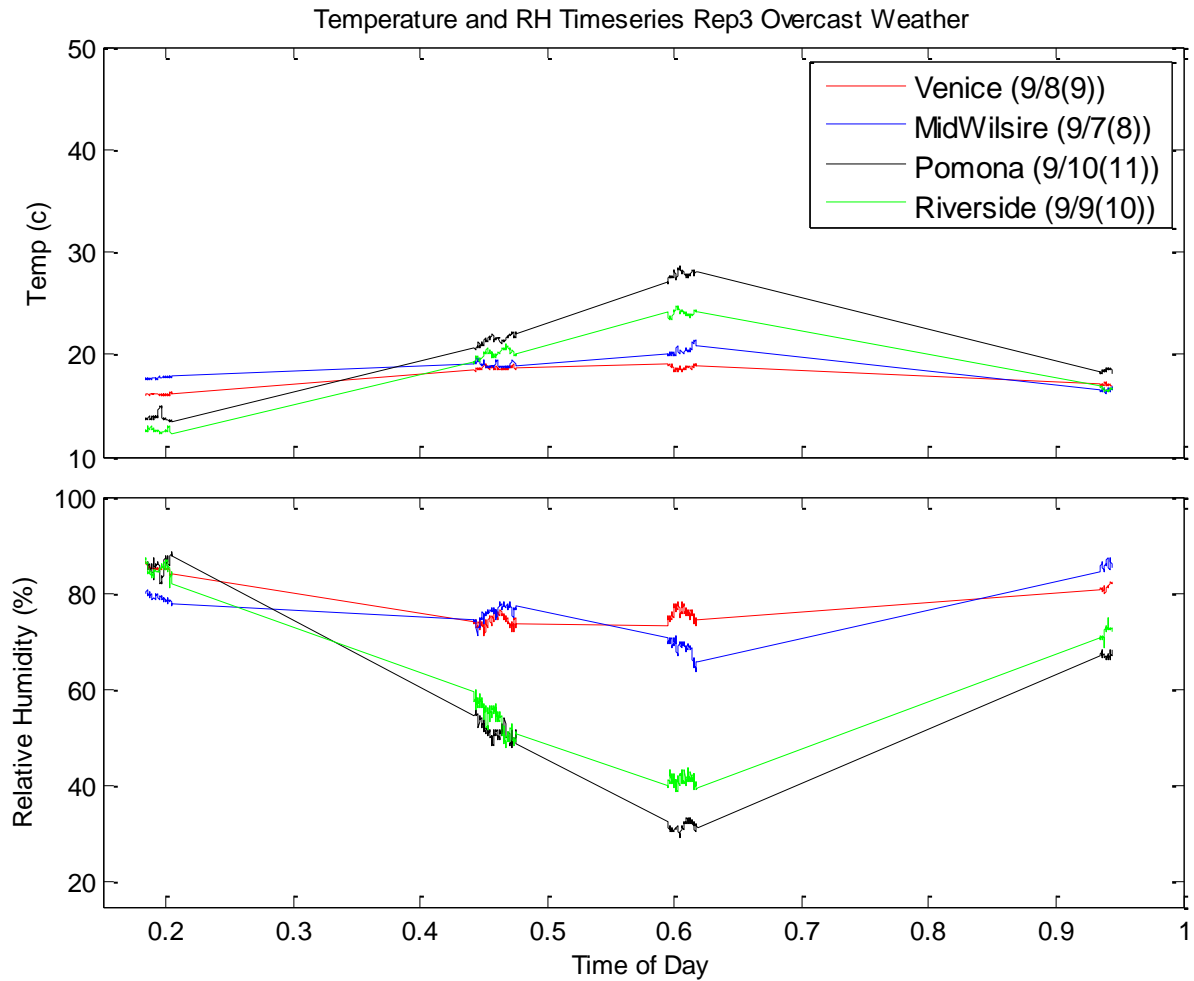
Figure 6 Comparison of the temperature and relative humidity (RH) for each run for repetition 3 over all measured locations during overcast weather

The direct relationship between temperature and RH can be further seen through the regression between the two variables. Rep 3 is chosen to exemplify the trends between temperature and RH. As seen previously, the relationship between temperature and RH varies between each neighborhood. The relationships are best modeled using a quadratic regression. While there is a clear relationship (p-value < 0.05), there are still many other factors, causing r^2 values to be low in some cases. Over Riverside, the strongest correlation is shown during the10am run with an r^2 of 0.61 (figure 7). The other three runs show much lower correlations

with r^2 values below 0.40. The highest RH values are found at the beginning and end of the day while the lowest RH occurs at 2pm. The slopes during the 10pm and 10am runs are significantly larger than the slope during 4am and 2pm. The RH during the 2pm run is very low and most likely reaches its equilibrium with the evapotranspiration of the area equaling the amount of moisture being carried into the higher atmosphere. Conversely, the air is almost saturated during the 4am measurements so that RH does not vary considerably.
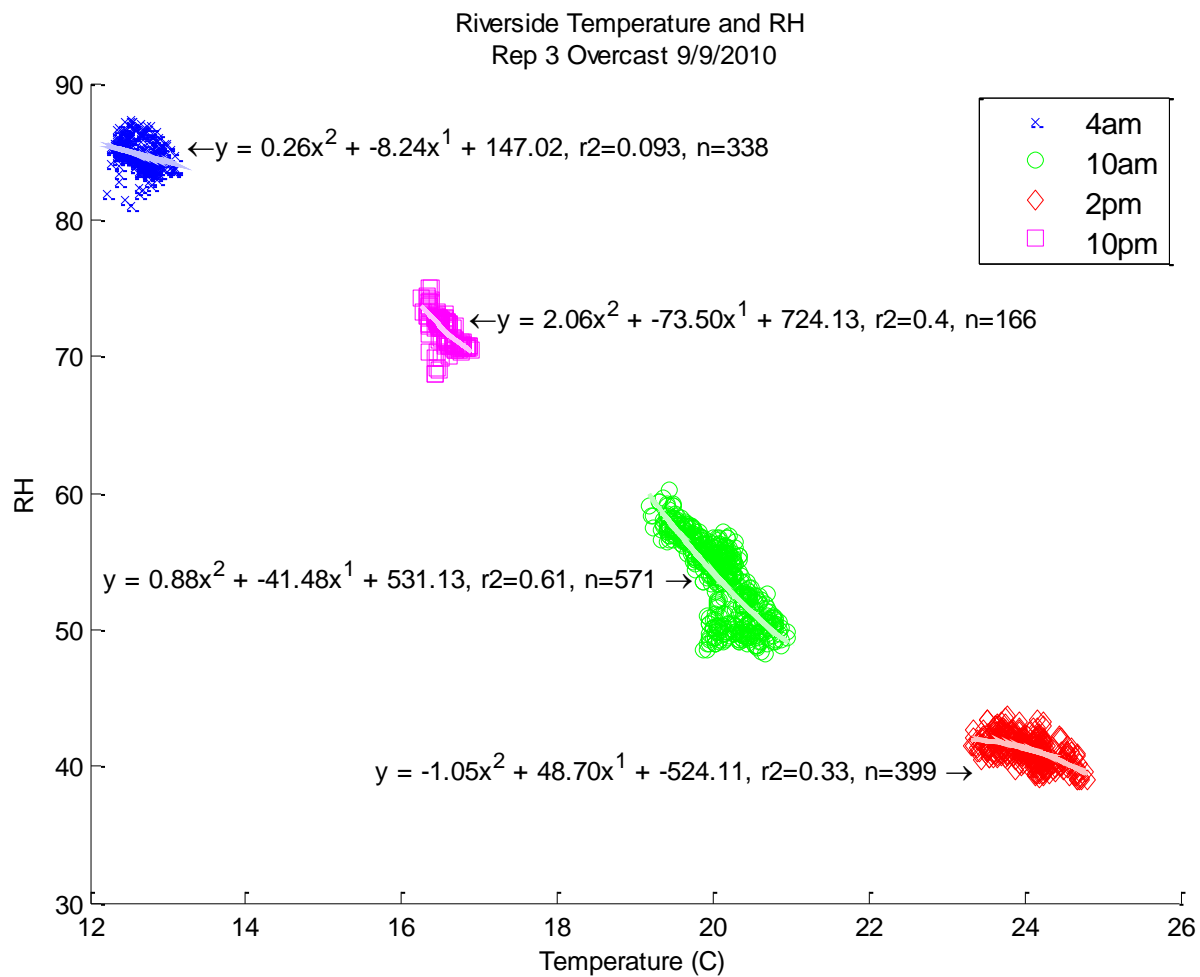
Figure 7 Regression of temperature vs. RH over Riverside for Rep 3 during overcast weather

In Pomona, the two earlier runs have higher correlation confidences between RH and temperature than the afternoon and evening runs (figure 8). Similar to the relationships seen over Riverside, the 10am and 10pm runs have large slopes. However, in this case, the morning measurement has a comparably large slope, indicating change earlier in the day.

Pomona Temperature and RH
Rep 3 Overcast 9/10/2010

←$y = 1.42x^2 + -42.88x^1 + 406.86$, r2=0.52, n=359

←$y = 4.76x^2 + -177.45x^1 + 1721.85$, r2=0.37, n=166

$y = 0.63x^2 + -30.48x^1 + 415.42$, r2=0.84, n=571→

$y = -1.96x^2 + 108.29x^1 + -1464.12$, r2=0.22, n=399 →

x   4am
○   10am
◇   2pm
□   10pm

RH
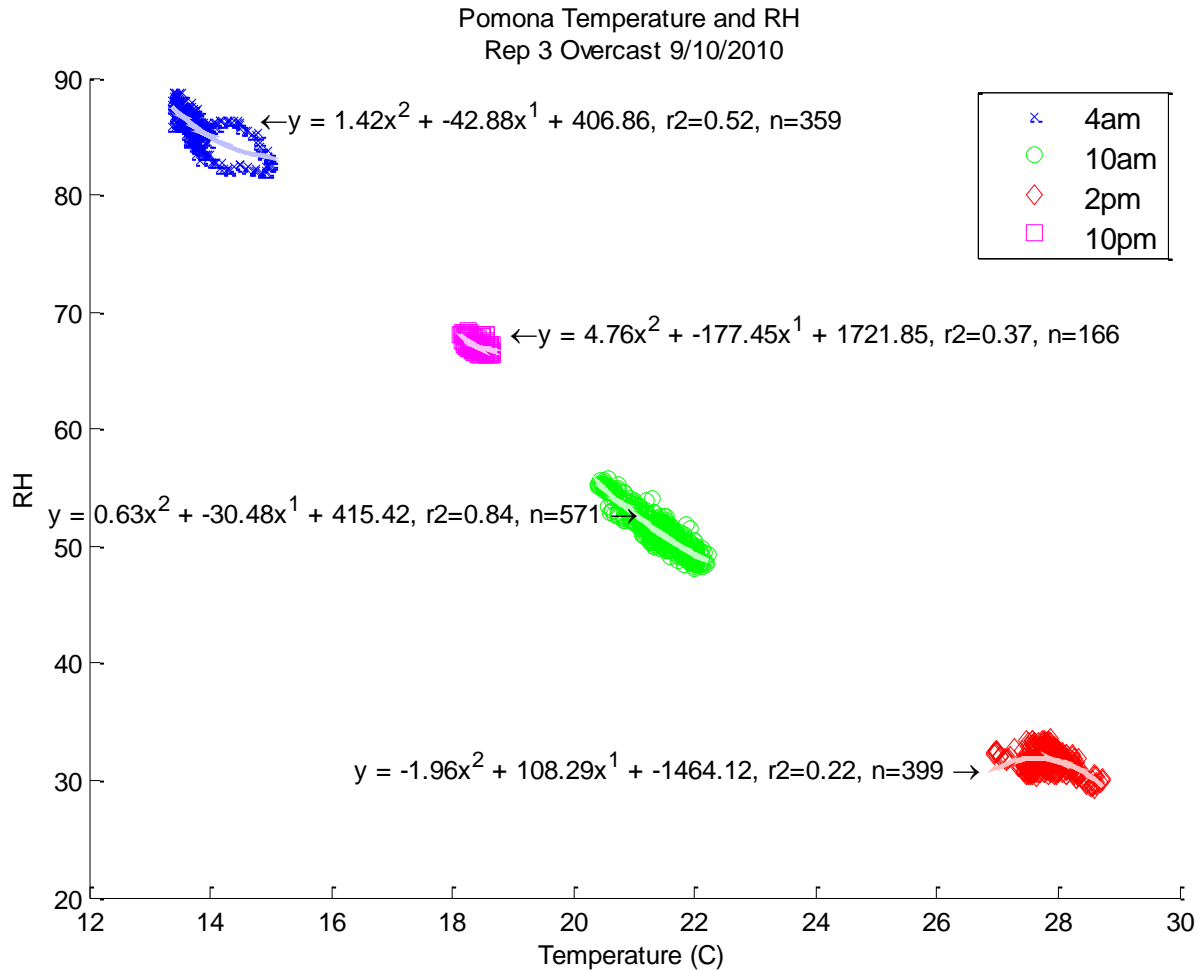
Temperature (C)

Figure 8 Regression of temperature vs. RH over Pomona for Rep 3 during overcast weather

Measurements over Mid-Wilshire show a stronger correlation between temperature and RH than in Riverside and Pomona (figure 9). With the exception of the 4am run, there is a high confidence of correlation between the RH and temperature ($r^2 > 0.5$). Interestingly, the slopes of

each of the regressions are similar over every measurement time. The range of RH change is not as large as the other neighborhoods so that even at the 2pm run, there are still large amounts of moisture in the air. Influence of the coast may allow for RH levels to stay higher and therefore not reach equilibrium at any point of the day. Instead, the air is constantly replenished by the vegetation of the area as well as evaporation from the ocean. It is also interesting that the 10pm run has a lower temperature and higher RH than the 4am run. Typically, 2pm is the hottest, driest run while 4am is the coldest, most moist run. This is most likely due to the ocean as an available water source. Because the ocean is readily available at the Venice location, once the temperature reaches a certain point, evapotranspiration rates will increase and allow moisture to return to the air much earlier than in previous cases. The heat allows the air to become moister by 10pm than it had originally been in the morning.
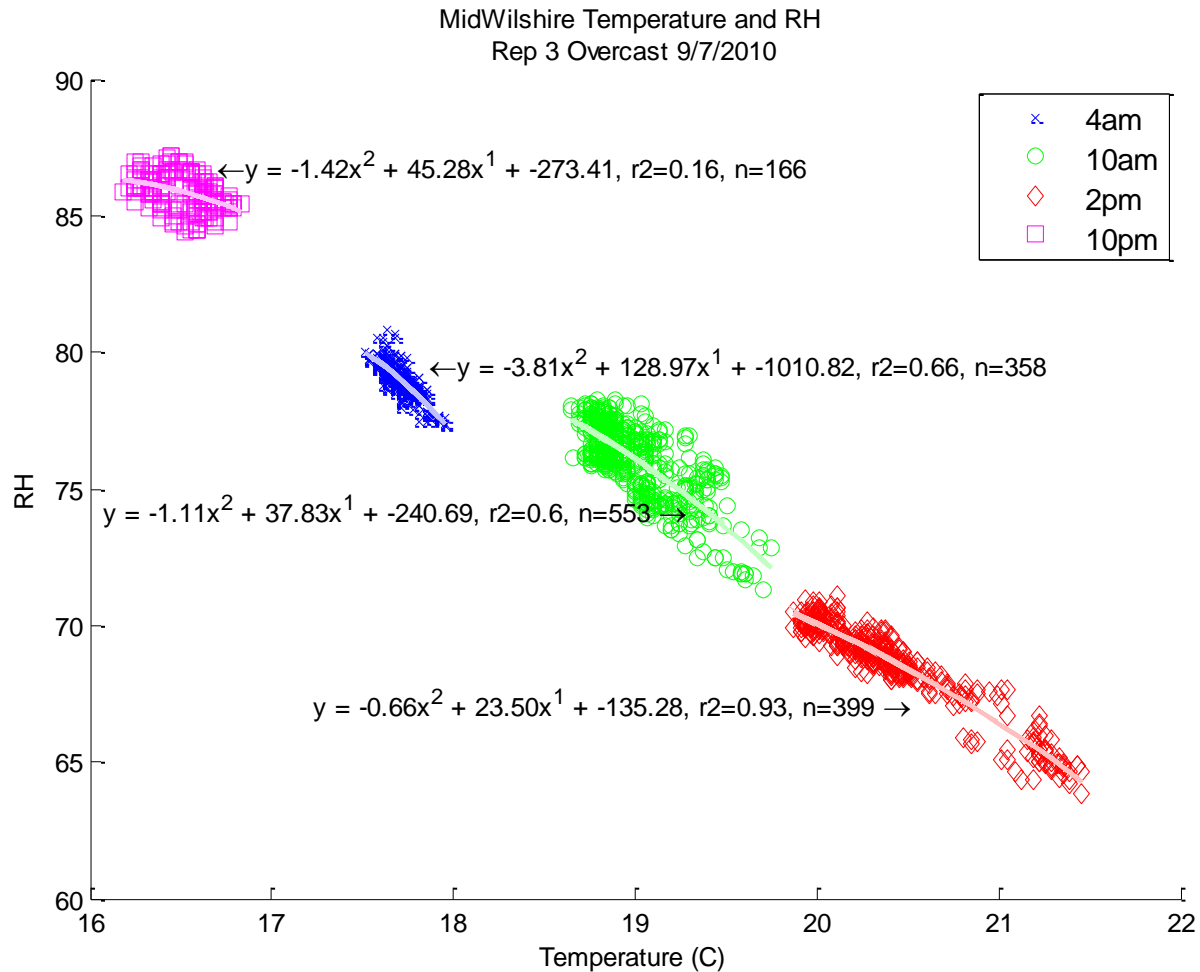
Figure 9 Regression of temperature vs. RH over Mid-Wilshire for Rep 3 during overcast weather

Of the three repetitions over Venice, the overcast weather shows the lowest confidence in correlation between RH and temperature (figure 10). Unlike the locations which are farther inland, there are more water sources that allow recharge of air moisture. The temperature and RH in this location are most likely affected the most by sea breeze and other climate variables that are associated with ocean currents. Interestingly, the temperatures during the 10am and 2pm run almost completely overlap though the RH experienced is different than what is expected. The RH values during the 2pm run are higher than those of the 10am. This shows a recharge of moisture in the air earlier than experienced in any of the other locations or cases. Similar to the

explanation given near Mid-Wilshire for atmospheric moisture recharge, this trend is most likely due to the ocean as an available water source. Even the mild heat increase by 10am causes evaporation over the ocean so that RH begins replenishing much earlier in the day.

Comparing the different repetitions over all locations there is a clear increase in the correlation between RH and temperature closer to the coast. As briefly discussed before, this is most likely due to the mediating effects of the coast. Inland locations experience water sources as a limiting factor in the variations of RH. The ocean also regulates the temperature for nearby costal locations because of its high heat capacity.
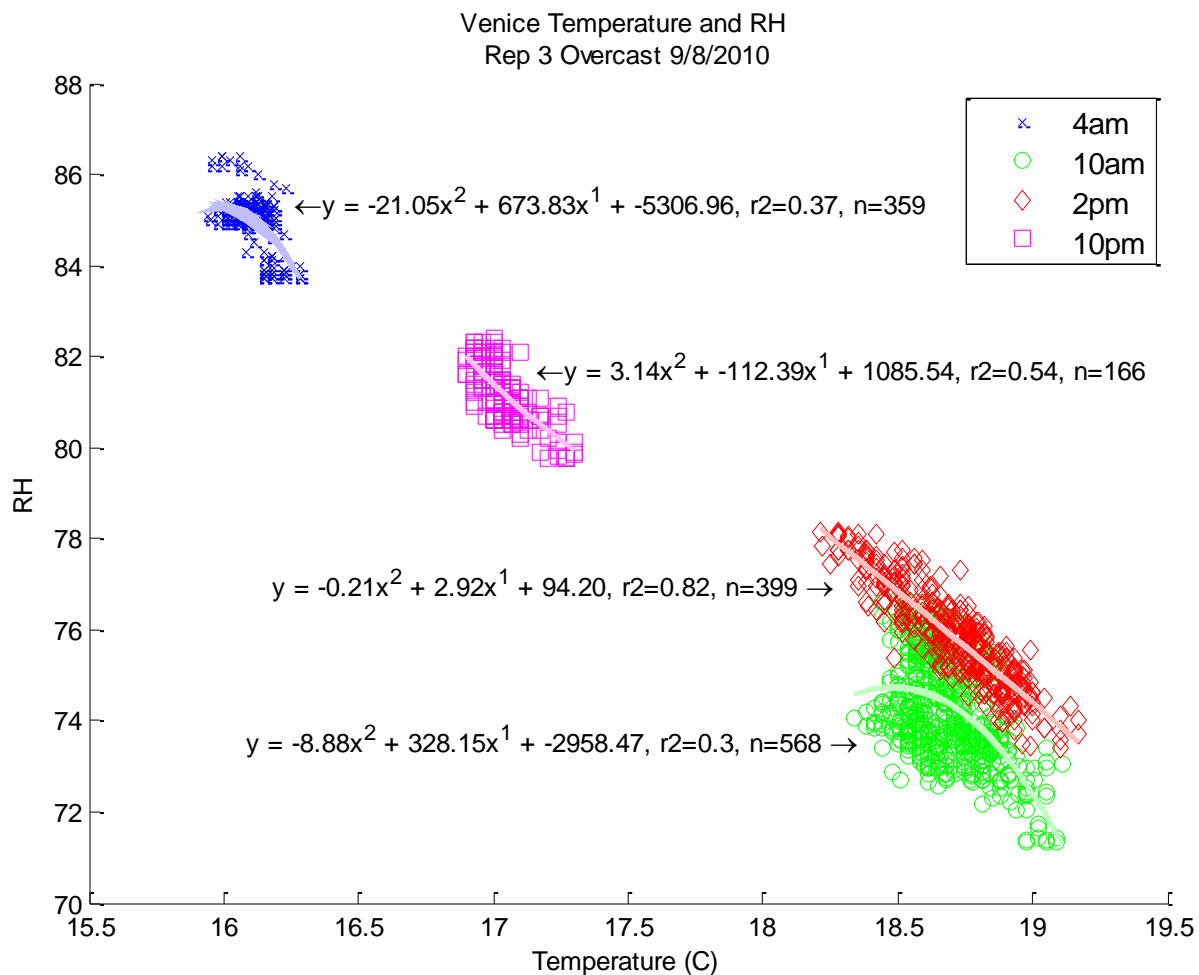
Figure 10 Regression of temperature vs. RH over Venice for Rep 3 during overcast weather

Temperature and Land Cover/NDVI Comparison

Hour 14 was chosen for this analysis because trends in figures 4 through 6 show the strongest differences over the four neighborhoods during this midday run. This is also the time at which the heat over the urban land scape is the most extreme. The influence of NDVI varies amongst the four neighborhoods as well as the weather conditions of the day that the data were collected. Figures 11 through 13 summarize the temperatures that were recorded during the different weather conditions; mild, heat wave, and overcast weather. As expected and discussed earlier, figure 11 (a) shows obvious increases in temperature as the distance from the coast increases, showing a significant coastal influence.
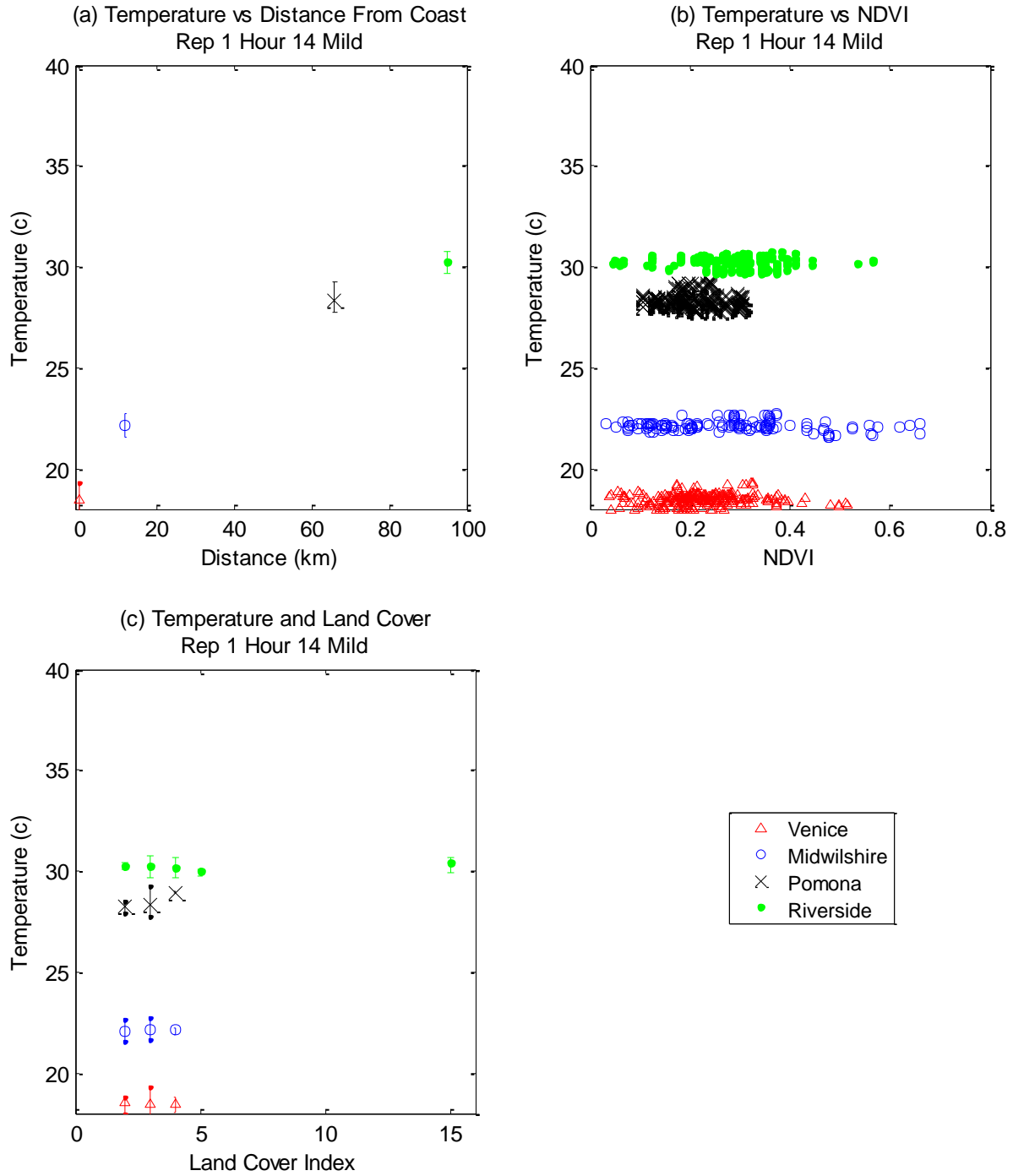
Figure 11 Temperature Comparisons with Distance from Coast, NDVI, and Land Cover for Rep 1 Hour 14. (a) and (c) display mean measured temperatures with the minimum and maximum range.
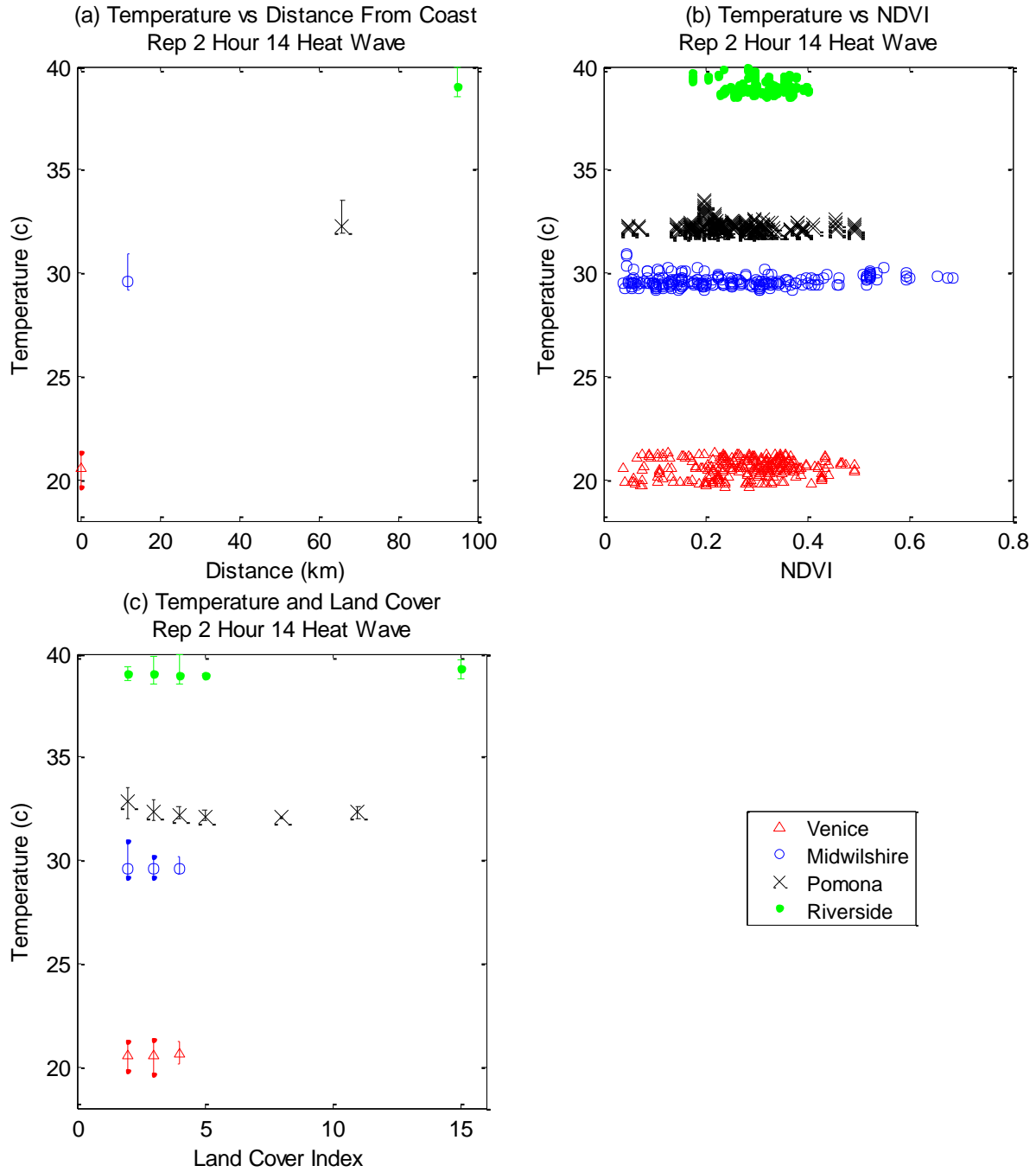
Figure 12 Temperature Comparisons with Distance from Coast, NDVI, and Land Cover for Rep 2 Hour 14. (a) and (c) display mean measured temperatures with the minimum and maximum range.
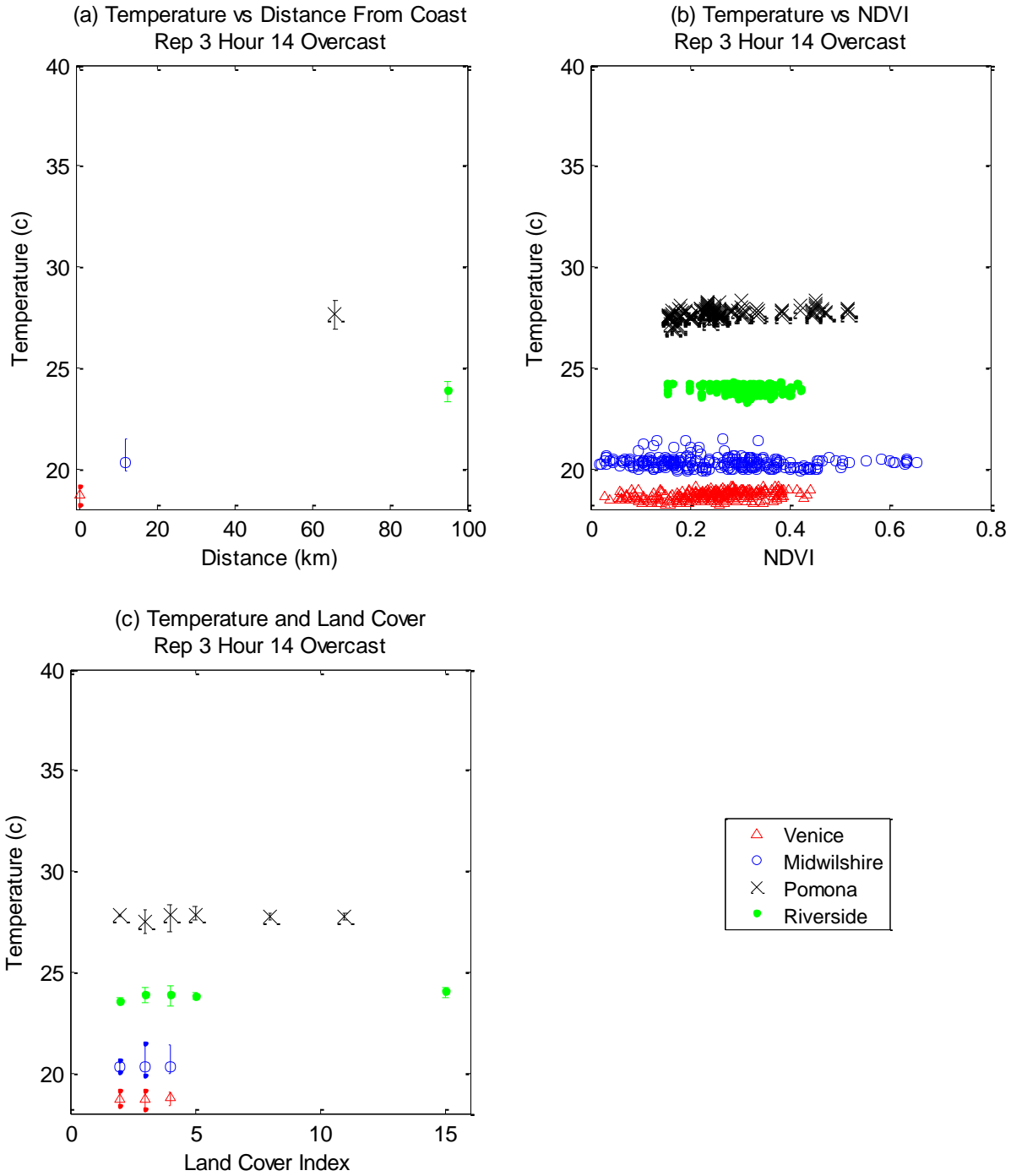
Figure 13 Temperature Comparisons with Distance from Coast, NDVI, and Land Cover for Rep 3 Hour 14. (a) and (c) display mean measured temperatures with the minimum and maximum range.

At first glance, (b) and (c) of the figures do not visually show a strong trend between

NDVI and temperature. Regression analysis of land cover indices showed low statistical

significance (p > 0.5) in all cases and was therefore not included in the analysis. Table 6

summarizes the regression statistics for both cases of temperature and RH with respect to NDVI

over every neighborhood and for every repetition. In both cases of temperature and RH there are

low correlations with low r^2 values. However, in most cases the results for p-values show strong

statistical significance implying that while NDVI may affect the temperature and RH at a micro

scale, there are many other factors that must be considered to create a confident regression.

Table 6 Temperature and RH vs. NDVI Regression Statistics for Hour 14

Neighborhood	Rep	Temp		RH	
		R^2	P-Value	R^2	P-Value
Venice	1	0.0085	0.0925	0.0355	0.0005
	2	0.0123	0.0518	0.0186	0.0165
	3	0.1467	0.0000	0.1421	0.0000
Mid-Wilshire	1	0.0390	0.0082	0.0466	0.0038
	2	0.0372	0.0013	0.0013	0.5560
	3	0.0182	0.0215	0.0008	0.6376
Pomona	1	0.0023	0.4167	0.0385	0.0008
	2	0.0174	0.0225	0.0442	0.0002
	3	0.1577	0.0000	0.0249	0.0187
Riverside	1	0.0055	0.2055	0.0005	0.6892
	2	0.0239	0.0120	0.0001	0.8844
	3	0.0096	0.0830	0.0180	0.0177

A multiple regression analysis was conducted to take into account the distance from the

coast (with the average latitude and longitude of Venice representing the coastal area). These

results showed much stronger correlations ($r^2 > 0.60$) with strong statistical significance from

both distance from the coast and NDVI except in the case of Rep 2, in which the NDVI p-value

was greater than 0.05. In this case, the distance from the coast has a strong influence on the

temperature and RH in the area. Specifically in Rep 1, the correlation including both distance

from coast and NDVI has an r^2 of over 0.90. The high p-value during Rep 2 may have been

because of the extreme heat which was taken during heat wave weather conditions. Past

observations by Stabler et al. (2005) also showed NDVI having less influence on climate

variables during higher temperatures.

Table 7 Temperature and RH vs. NDVI and Distance from Coast Multiple Regression Statistics for Hour 14

Repetition	Temp			RH		
	R^2	P-value		R^2	P-Value	
		Dist. from coast	NDVI		Dist. from coast	NDVI
1	0.9650	0	0.0001	0.9367	0	0.0003
2	0.8311	0	0.1856	0.6647	1.01E-273	1.98E-05
3	0.6457	3.71E-253	0.0027	0.8243	0	4.06E-05

Data were also analyzed for hour 4 at which the experienced the lowest measured

temperatures. Similar to what was observed in the study by Stabler et al. (2005), data from hour

4 showed a stronger influence of land use than in hour 14. Table 8 shows a summary of the

multiple regression analysis that was made for hour 4 over the individual neighborhoods. For the

majority of cases, the land cover (LC) showed strong statistical significance ($p < 0.5$). However,

NDVI showed less statistical significance than during hour 14 with an overall increasing

significance when traveling away from the coast (Venice to Riverside).

Table 8 Temperature and RH vs. NDVI Regression Statistics for Hour 4

Neighborhood	Rep	Temp			RH		
		R^2	P-value		R^2	P-Value	
			LC	NDVI		LC	NDVI
Venice	1	0.0829	9.3E-06	0.8064	0.0583	0.0018	0.0032
	2	0.5326	2.5E-46	0.3028	0.4858	9.95E-41	0.3884
	3	0.0042	0.4877	0.3080	0.0214	0.0274	0.2646
Mid-Wilshire	1	0.2539	1.7E-17	0.0140	0.1319	2.15E-08	0.0034
	2	0.1204	1.8E-09	0.4167	0.0487	0.0003	0.2738
	3	0.0938	1.8E-06	0.0149	0.1424	2.09E-11	0.7689
Pomona	1	0.2786	0.0007	0	0.3061	0.0003	1.4E-05
	2	0.2301	0.0051	0	0.1074	0.8511	6.2E-07
	3	0.0047	0.3113	0.3705	0.0054	0.2343	0.4273
Riverside	1	0.0761	0.1402	0.0295	0.1175	6.59E-06	0.0273
	2	0.1771	9E-06	2.5E-08	0.3944	2.63E-14	1.4E-19
	3	0.2256	2.1E-10	0.0065	0.2165	4.10E-10	0.0038

Figures 11 through 13 (b) are visually relatively similar in terms of the dependence of temperature on NDVI. Figures 14 through 16 (a) and (c) highlighting hour 4 differ significantly from figures 11 through 13 (a) and (c) for hour 14. There is a clearer pattern of temperature decrease following increasing land cover index shown in (c) of the figures (table 8). The land cover indices help to categorize land use with lower numbers typically describing areas which have higher degrees of urban build up. Figures 14 through 16 (c) show clear decreases in the maximum and average temperatures as the land cover index increases over Venice and Mid-Wilshire. The regression is not as clear in the cases of Pomona and Riverside during Rep 2, which was confirmed by the statistics in table 9. The correlation seen in (a) of the figures describing temperature dependence on distance from the coast is not as visually distinct as during hour 14. The change in temperature traveling coast to inland differs from each repetition to the next with an overall decrease in temperature as discussed earlier.

Table 9 Temperature and RH vs. NDVI and Distance from Coast Multiple Regression Statistics for Hour 4

Rep	Temp				RH			
	R^2	P-value			R^2	P-Value		
		Dist. from coast	LC	NDVI		Dist. from coast	NDVI	LC
1	0.5896	6.43E-124	0.3456	0.0005	0.3431	4.48E-61	0.0019	0.0619
2	0.3609	3.27E-100	0.0040	0.6436	0.6259	3.12E-218	0.8903	0.0002
3	0.8029	0	0.6730	0.0132	0.1581	1.20E-40	0.0015	0.0198

Once again, a multiple regression was conducted for the temperature and RH over the coast to inland gradient taking distance into account. Tables 7 and 9 show changes in the correlation between temperature and RH and the three variables of distance from coast, NDVI, and LC. In the case of hour 4, LC plays a more significant role, both in each neighborhood and in the broad length from coast to inland with p-values close to or less than 0.05 in the case of RH and in one case of temperature. The significance of LC and NDVI tend to be opposite of each other, having higher LC significance with lower NDVI significance. The r^2 correlation was also less in the case of hour 4 than in hour 14 even when distance from the coast was taken into account. This suggests that the distance from the coast has less of an effect on the temperature and RH during the earlier times of the day. The difference in influence of land use and distance from the coast seen between hour 14 and hour 4 could be due to the complex geometric structure of the urban area. As discussed in several studies of UHI, urban canyons decrease airflow through a city and trap heat within the fabric of urban cover through the night when temperatures are typically lowered (Arnfield, 2003; Houet and Pigeon, 2001). Therefore, in the current study, land use shows increased influence on temperature and RH during the night and early morning hours. The increased role of land cover over a neighborhood scale from hour 4 to hour 14 may

also be due to the calm early morning conditions. During the hotter midday conditions, it is

likely that atmospheric mixing would dissipate effects of differing land cover.
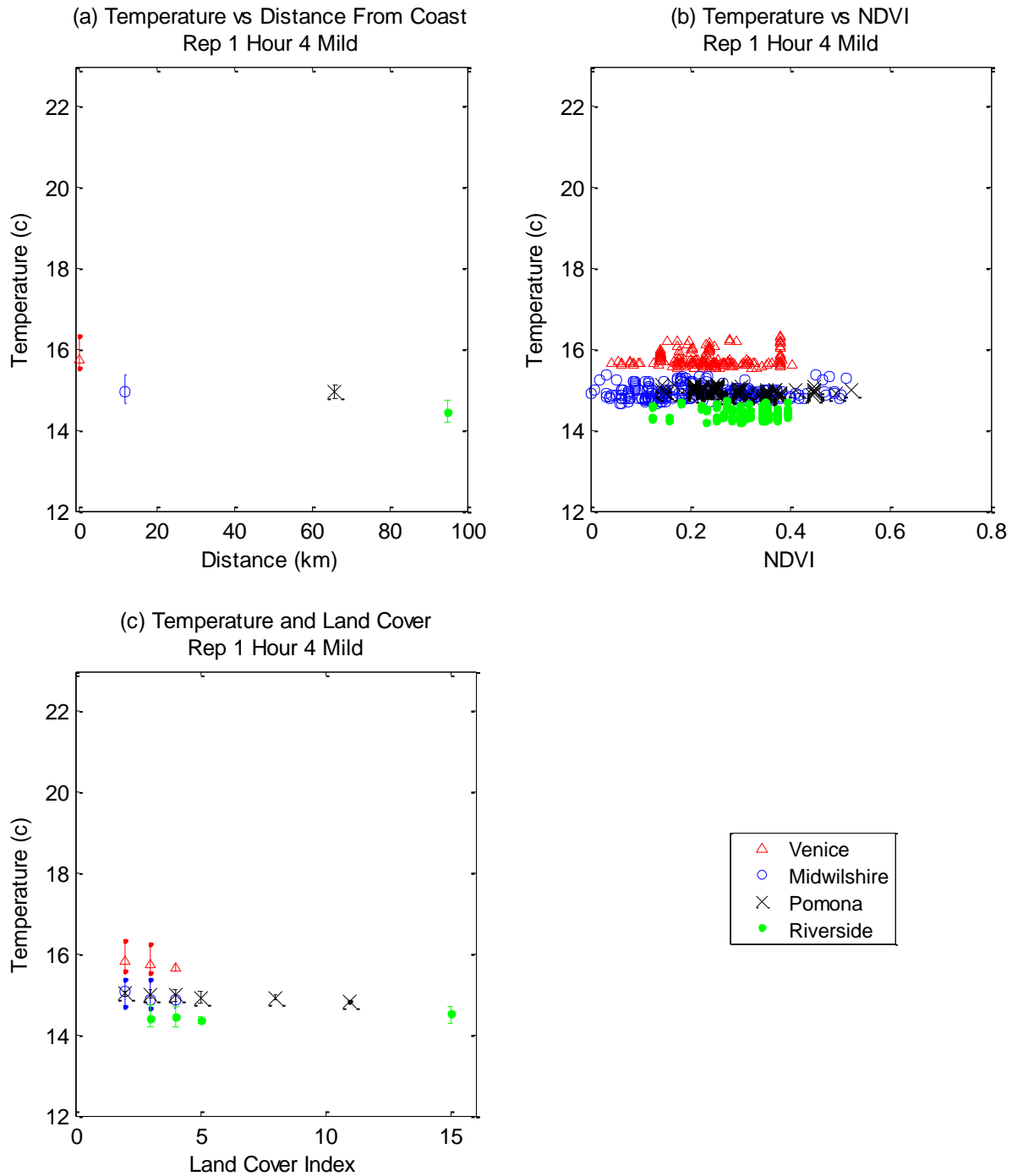
Figure 14 Temperature Comparisons with Distance from Coast, NDVI, and Land Cover for Rep 1 Hour 4. (a) and (c) display mean measured temperatures with the minimum and maximum range.
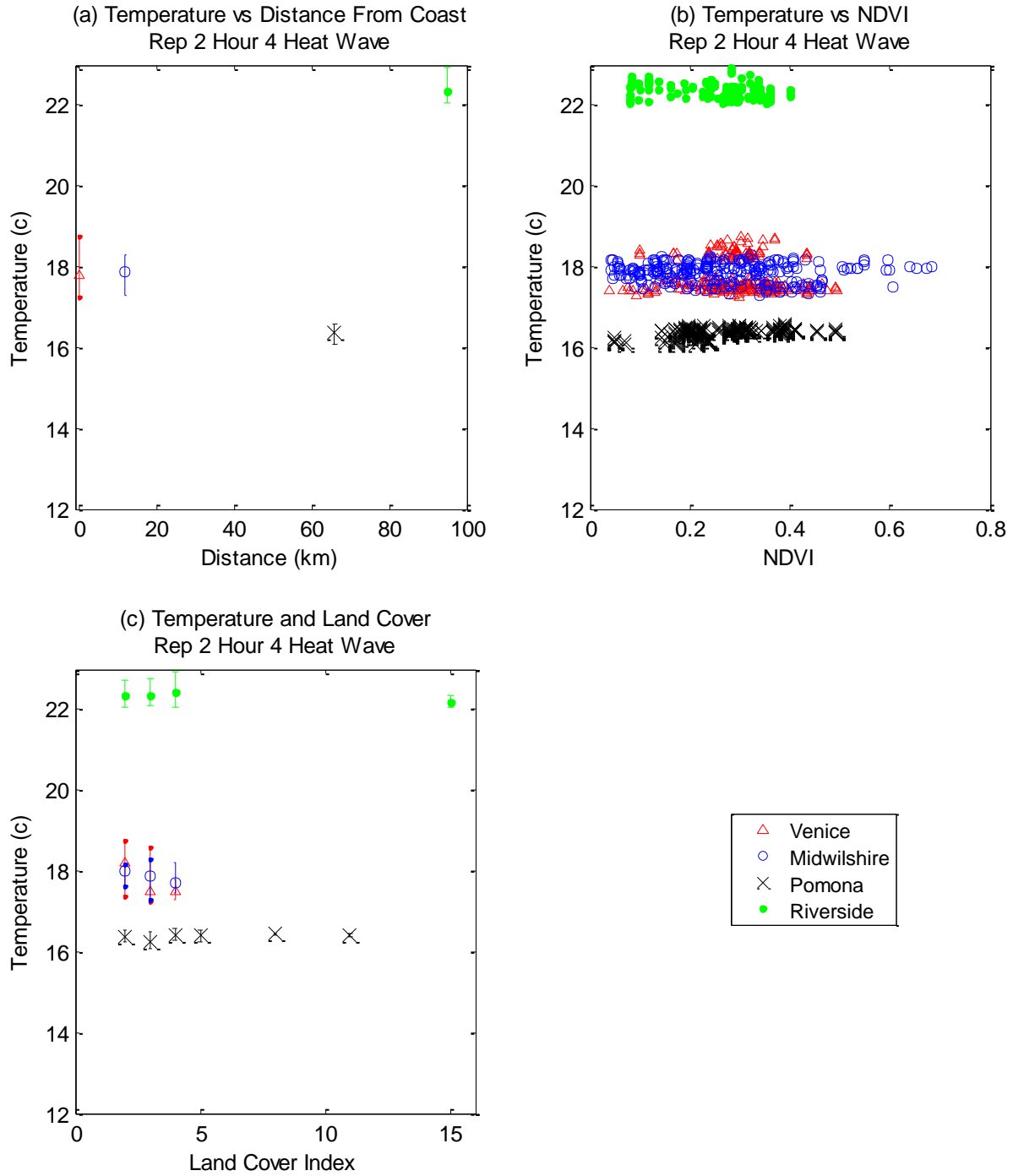
Figure 15 Temperature Comparisons with Distance from Coast, NDVI, and Land Cover for Rep 2 Hour 4. (a) and (c) display mean measured temperatures with the minimum and maximum range.
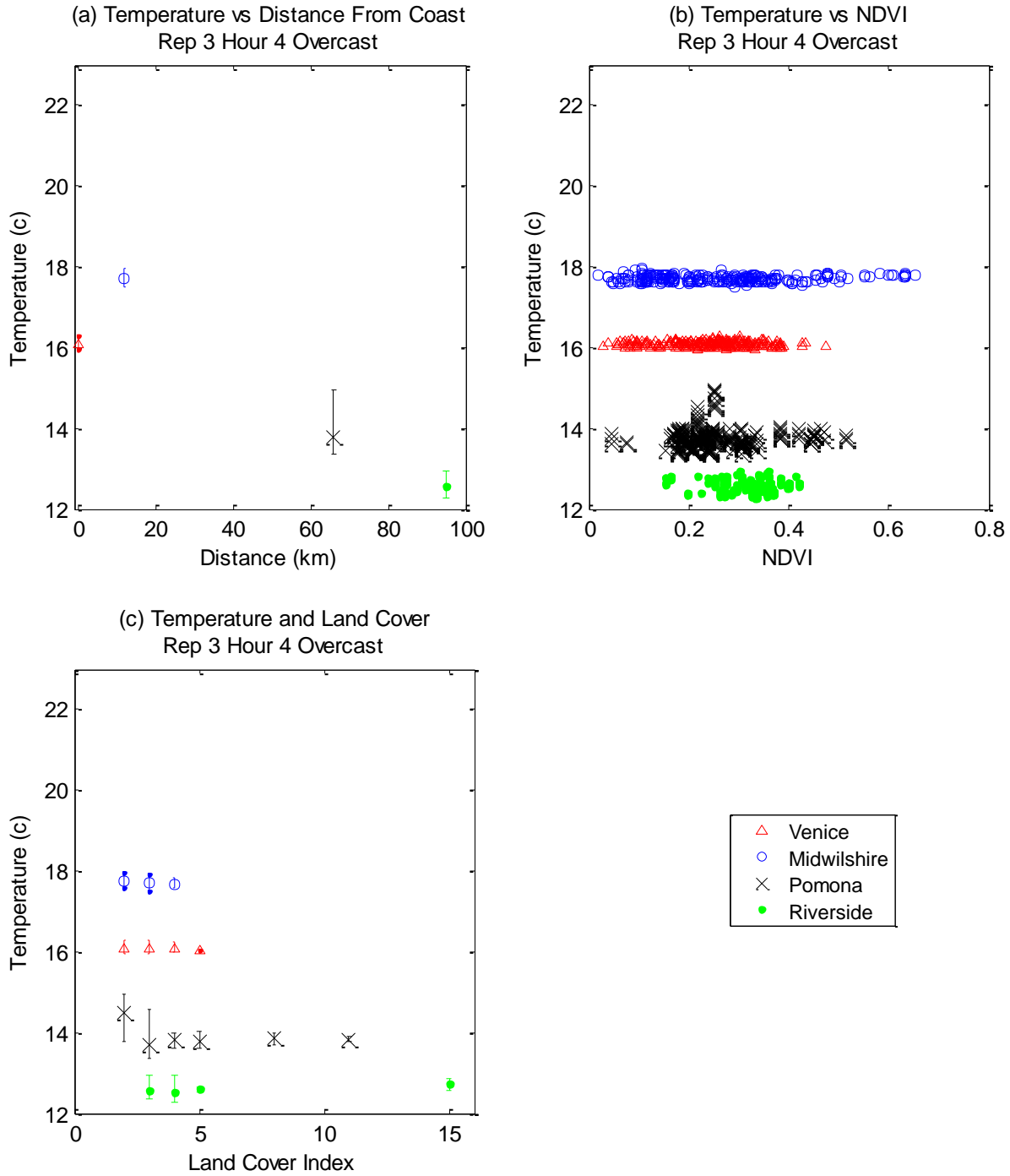
Figure 16 Temperature Comparisons with Distance from Coast, NDVI, and Land Cover for Rep 3 Hour 4. (a) and (c) display mean measured temperatures with the minimum and maximum range.

The correlation between land cover and NDVI and temperature and RH were lower than

expected at a neighborhood scale. This may be because differences between urban land cover

types are difficult to describe simply through the use of a land use index. There are many different factors of land use that can individually affect UHI including imperviousness, geometric structure, and even the material of the urban scape (Arnfield, 2003). The low correlation between temperature and vegetation or land cover in this case may also be due to the small spatial scale at which measurements were taken. The largest square area that was sampled was in the Pomona neighborhood with an area approximately 10km^2. This would cause temperatures to be affected by not only the land cover type at the sampling point but also in the close vicinity. From past temperature and vegetation studies, vegetation has shown to be at least one of many other factors affecting temperature (Arnfield, 2003; Brazel and Johnson, 1980; Grimmond et al., 1996; Stabler et al., 2005).

The observed relationships between temperature and relative humidity as well as vegetation and land cover show the influence of the coast on climate variables farther inland. Analysis through multiple regression showed that vegetation may only have a minor impact on temperature as compared to other variables. Typically vegetation has cooling effects on UHI because of the diversion of radiation towards the latent heat flux. In the case of coastal areas, there are many other sources of moisture that would allow for cooling that have stronger influences such as the marine layer. This would explain the increased significance of vegetation in the inland neighborhoods. The inland neighborhoods deplete moister gradients from the coast and rely on the vegetation in the area to hold in moisture for cooling. This was highlighted not only by the increased statistical significance of vegetation, but also the low RH over Riverside as seen in figure 5 earlier. It was also seen that instances of intense temperature causes vegetation to lose its cooling influence. In both cases of statistical analysis, the NDVI had strong statistical

significance over Rep 1 and Rep 3 (mild and overcast), but very weak significance during Rep 2 (heat wave).

Uncertainties and Assumptions

While efforts were made to make this study thorough and accurate in measurement and processing of data, important assumptions were made that could cause potential errors. Many of these uncertainties were described throughout various sections, but are summarized here as noted:

- Due to the nature of mobile measurement, not all data over the different transects were collected at the same day and time. As noted in table 4, each neighborhood was measured on different days. Consecutive days were chosen in order to keep the data as similar as possible; however, climate variables differ from day to day.

- Land cover type and usage was taken from CCAP index and are only overarching descriptions of land cover usage and cannot fully describe the many factors of an urban land scape. Both NDVI and land cover type were based off of satellite measurements at a 30m spatial scale that may also skew correlations between temperature and RH measurements that were taken at a finer scale.

- Because small neighborhoods areas were studied, some measurements may have been affected by tall buildings or street trees with spreading canopies so that temperature measurements were taken both in shade and out of shade. For this reason, averages, standard deviations, maximum, and minimums were all considered when analyzing the data.

- Errors were also incurred in use of the mobile measurement method. Because measurements were taken from a car in local traffic, there may have been instances of

slower or faster travel times. The data was logged methodologically and noted where

stops or heavy traffic was experienced. Extremes in data were removed as discussed

in the methods and data were removed where there were surroundings that may have

heavily skewed the data. Also because of the removal of these data points, the

measured points in each transect from each repetition and every run were not exactly

the same, but followed the same general paths.

- The measurement tools themselves also incur error. The limitations of the probe used
  for data collection are listed in the methods section.

Conclusions/ Future Study

The current study measured the variability of temperature and relative humidity of four

urban neighborhoods spanning from the coast of Los Angeles to the Eastern edge of Riverside

during three different weather conditions in order to examine (1) the influence of local vegetation

and land cover type over a diverse set of neighborhoods and (2) moderation of the studied

variables by the coastal climate across the urban gradient. Several key conclusions can be drawn

from the current study:

- Temperature trends from coast to inland vary at the hourly scale and are dependent on
  general regional weather conditions. On average, the temperature increases as the study
  area is farther inland. However, coastal areas have a smaller range of maximum and
  minimum temperatures because of moderation by the ocean. Heat wave weather makes
  the differences in temperatures between neighborhoods more pronounced while overcast
  weather moderates the temperatures changes.

- Influence of the coast and land cover usage on the climates over the neighborhoods varies
  throughout the day. During earlier hours of the day, the influence of the coast is lessened

41

while land usage plays a slightly larger role in temperature variations. During midday, the distance from the coast is an extremely strong variable in temperature determination while the effects of land usage become insignificant. Similarly, during the extreme heat conditions during Rep 2, the influence of land usage and NDVI become negligible.

- Overall, temperature trends in Riverside differ from the other three neighborhoods, indicating that it may be outside or on the edge of coastal influence. During hour 4, Riverside has the hottest temperature during Rep 2 and the lowest temperature during Rep 3, showing extreme variability in temperature. In these cases it does not follow the typical temperature trend observed in the other three study neighborhoods. During Rep 2 the Riverside neighborhood is the only of the four to not recover its relative humidity at the end of the day. The strongest statistical significance of vegetation on temperature is found over Riverside, implying less coastal influence on temperatures and stronger influence of its own microclimate and land usage.

The current study provides a starting point for continued research in urban heat over coastal areas. To better understand the influence of land usage in combination with coastal effects, measurements focused on specific urban geometry and land cover may be needed. As described, there are multiple characteristics of urban cover that effect temperature gradients beyond what indexing land cover types can prove. It is also difficult to confirm many of the trends seen in the data because there is only one data set per repetition and run. Weather is extremely variable and though measurements were taken in consecutive days for each repetition, there are obvious uncertainties in measuring temperature and relative humidity gradients over several days. Observed characteristics such as the change in land usage dependence over the

three repetitions, the hotter temperature in Pomona over Riverside during Rep 3, or the extreme low in relative humidity over Riverside during Rep 2 cannot be completely confirmed as what will typically occur on heat wave or overcast days. In addition to mobile transect measurements, other methods of temperature can be evaluated over the area such as satellite and fixed station data. As mentioned before, both have limitations, but also allow for less intensive means of data collection. Additional research of these areas can help to determine the temperature threshold or related factors that cause vegetation or land cover usage to become inconsequential to temperature gradients. In the study of urban heat islands (UHI) and determining how to best mitigate extreme heat, it is important to fully understand all factors relating to it. As of now, one of the leading methods of mitigating UHI is through increased vegetated areas. However, if there is a threshold at which vegetation can no longer cool an area, research must be done to find other avenues of reducing urban heat. Re-sampling of the same transects will help to not only confirm the observations described here, but will also increase knowledge of the growing urban heat at a longer temporal scale. As exemplified by continued mobile transect studies over Phoenix, Arizona, long term research using mobile transects over an area can give a much fuller understanding of the climatological characteristics over an area (Brandsma and Wolters, 2012; Hedquist and Brazel, 2006; Stabler et al., 2005).

Future study may also include measurements over different seasons. Research by others, such as Sun et al. (2009), have shown the importance of measuring effects of urban heat not only during the summer months when extreme heat events occur, but also during the winter months which have been warming due to increased anthropomorphic sources such as heating systems. From the information presented here, it is apparent that there is a large influence of the coast on the temperature gradients that affects not only the strength of UHI, but also the effect of

vegetation and land cover over a significantly large area. The continued growth in population and urban cover over Los Angeles necessitates the continued study of the coastal and land cover influences on temperature variability and extreme heat.

Appendix

Appendix A: Measured and Station Data Comparison

The figures below show the time series of collected data and the progression of temperature and RH as the car traveled through each transect from coast to inland. The figures allow better visualization of the days which the data was collected. These figures also compare the measured mobile met data with station data taken from the National Climatic Data Center (NCDC) ran by the National Oceanic and Atmospheric Administration (NOAA) and the California Irrigation Management Information System (CIMIS) ran by the Department of Water Resources Office of Water use Efficiency in California. For each repetition, the station data and mobile met data are relatively similar. There is a margin of error for the comparison of the station data because of the difference in measuring location. In some cases the station data seems to be shifted over time from the mobile met data. The station data is not always reliable and has missing data during some of the measurement times. The station names and locations are found in table 10.
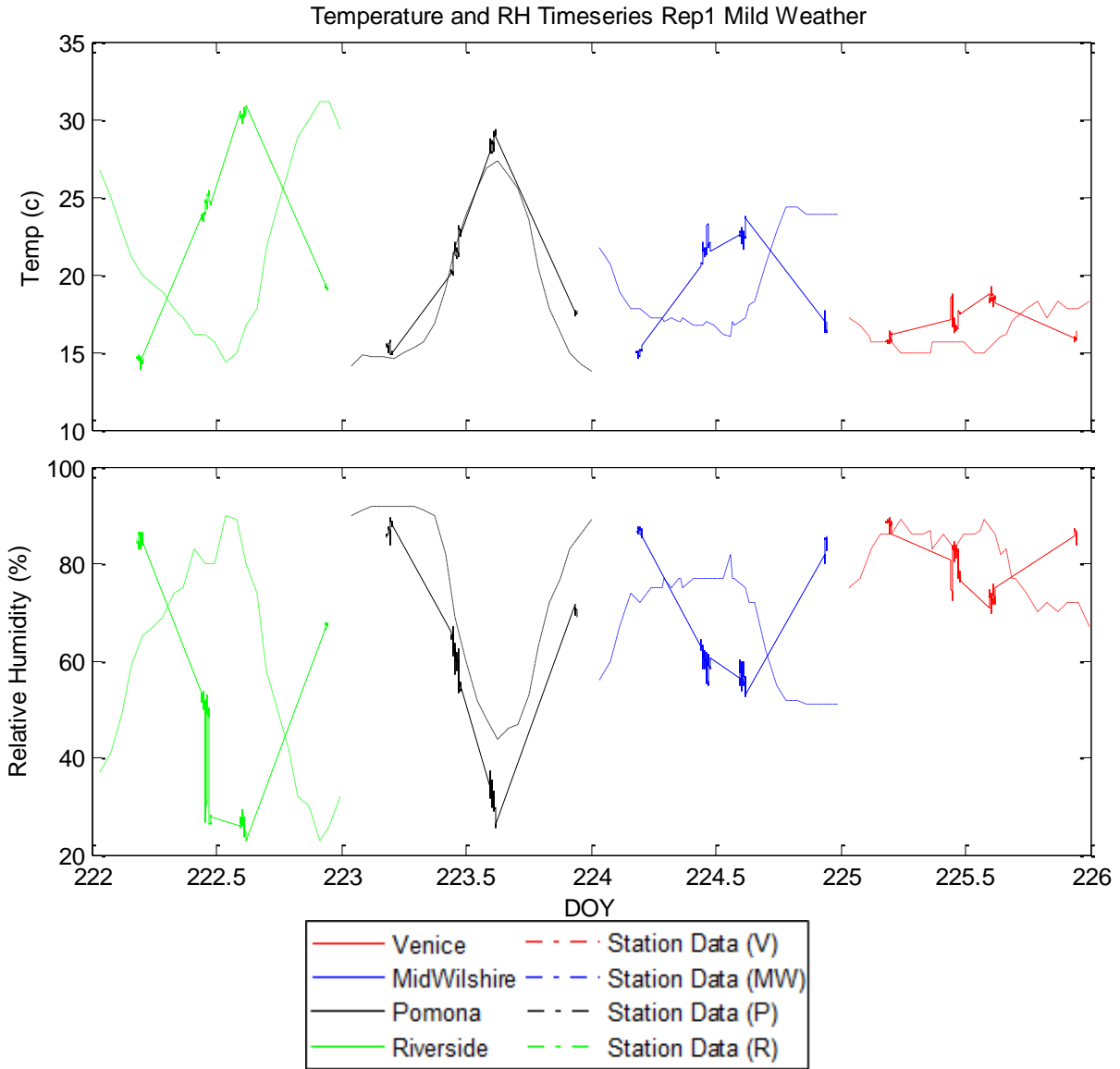
Figure 17 Comparison of the time series of all runs and locations for temperature and RH between mobile met measured data and known station data for Rep 1 during mild weather
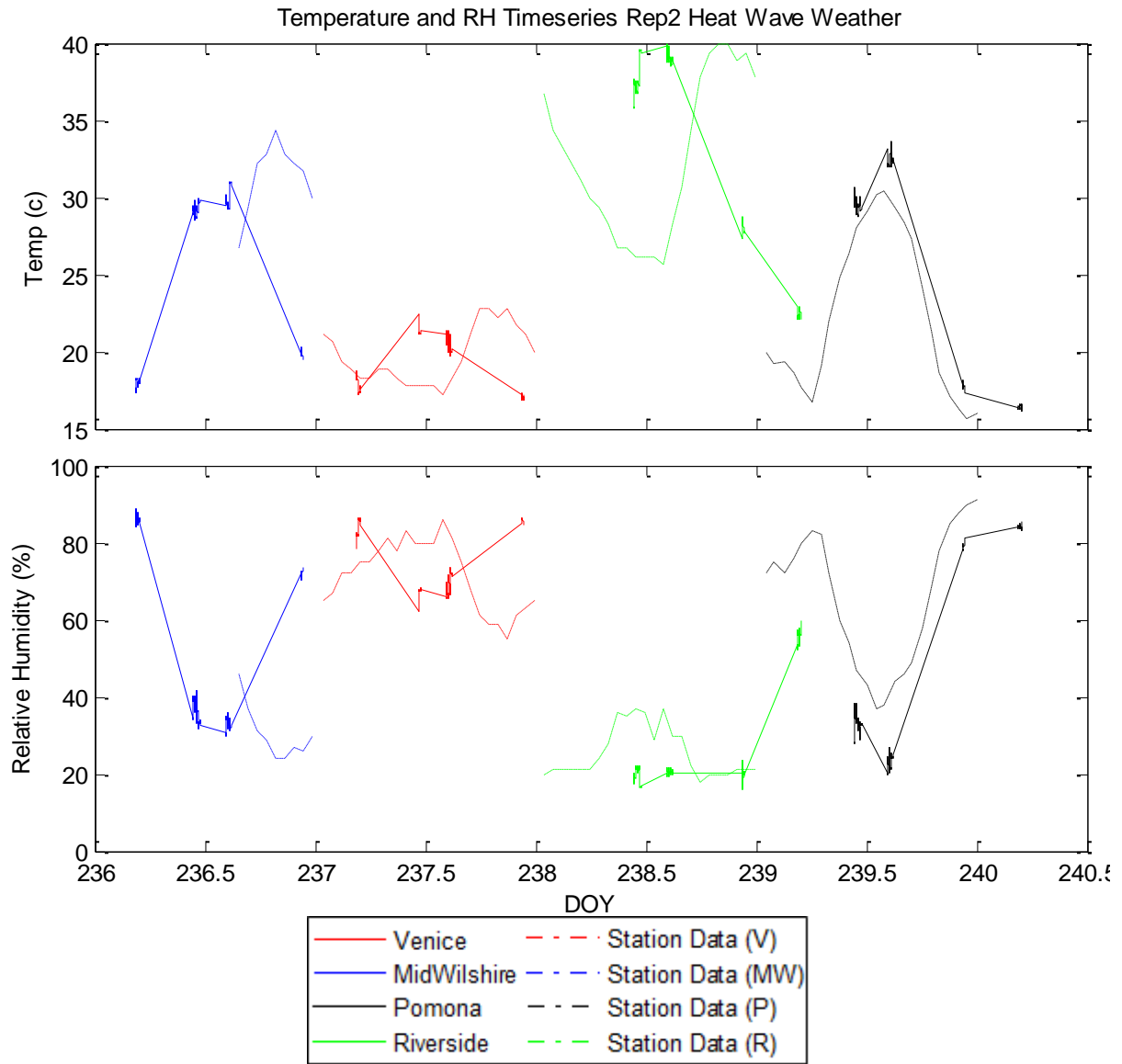
Figure 18 Comparison of the time series of all runs and locations for temperature and RH between mobile met measured data and known station data for Rep 2 during a heat wave
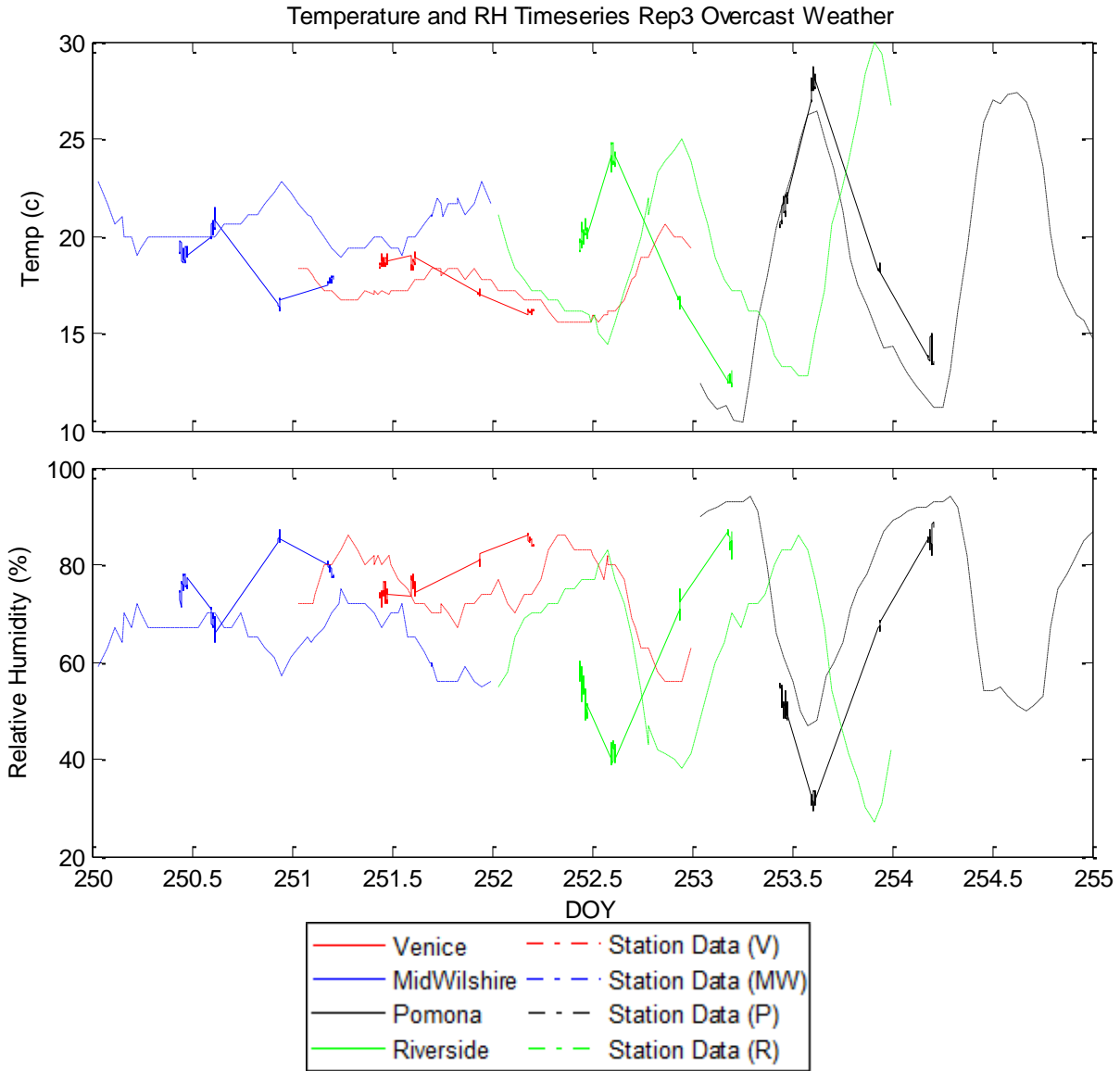
Figure 19 Comparison of the time series of all runs and locations for temperature and RH between mobile met measured data and known station data for Rep 2 during overcast weather

Table 10 Station Names and Locations

Station Name	Neighborhood of Compared Measurement	Latitude, Longitude
Santa Monica	Venice	34.016, -118.451
USC	Mid-Wilshire	34.051, -118.235
#78*	Pomona	34.056, -117.813
Riverside	Riverside	33.952, -117.439

* CIMIS station data used because of lack of data in NCDC database

Appendix B: Mobile Measurement Data Boxplots
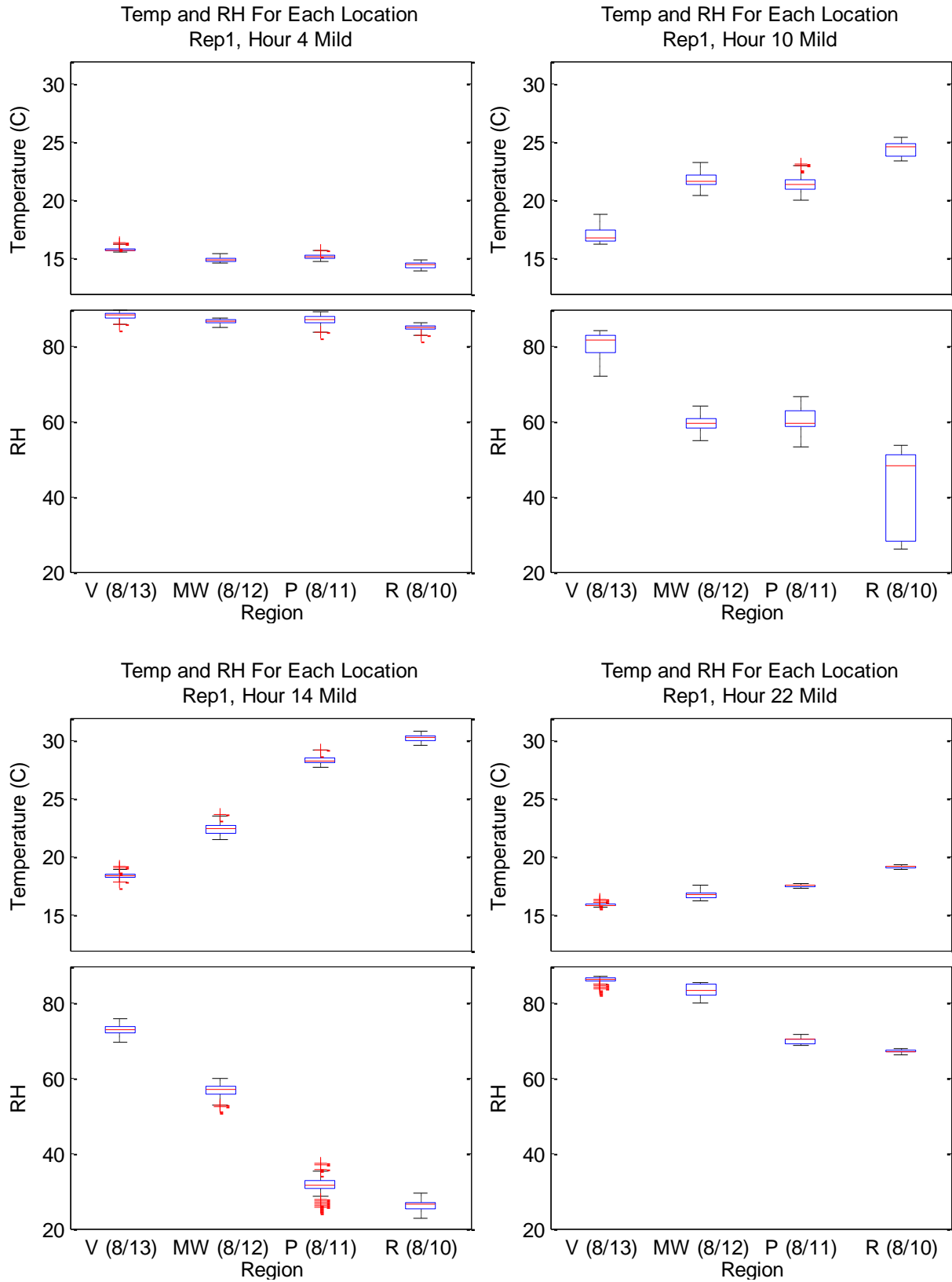
Figure 20 Temperature and RH Box Plots Rep 1
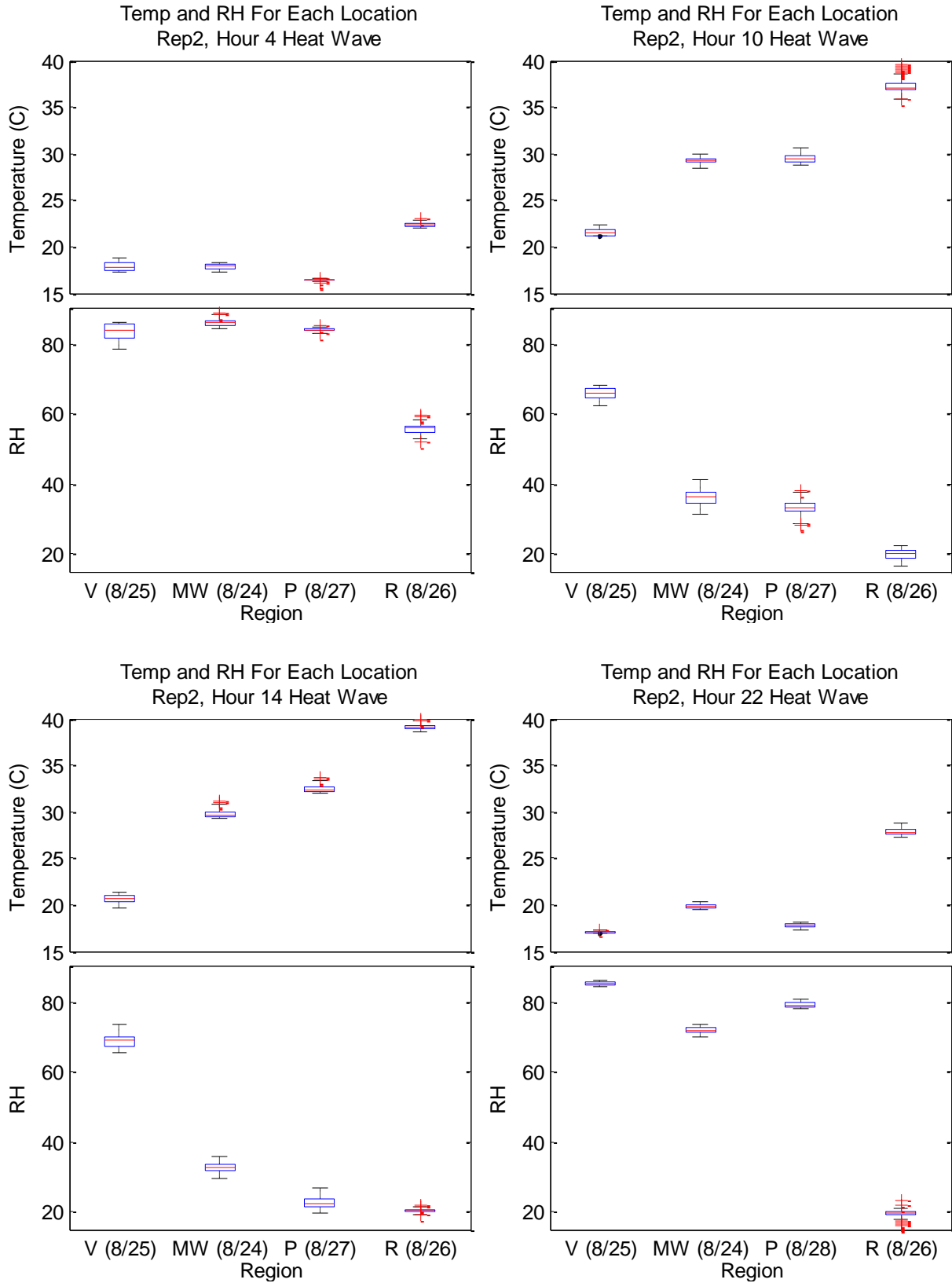
Figure 21 Temperature and RH Box Plots Rep 2

Appendix C: Temperature and Relative Humidity Regression

The relative humidity (RH) varies inversely with the temperature as shown by the negative sloping correlations. Over Riverside Rep 1, the strongest correlation is shown during the 2pm run with an r^2 of 0.68. The other three runs show relatively low correlations with r^2 values below 0.50. The highest RH values are found at the beginning and end of the day while the lowest RH occurs at 2pm, which is expected. The slope of the regression at 2pm is also more apparent than during the other runs. During mild weather, the variance of RH and temperature follow a relatively linear or elastic pattern, decreasing during the day and returning to a higher RH and lower temperature in the evening.
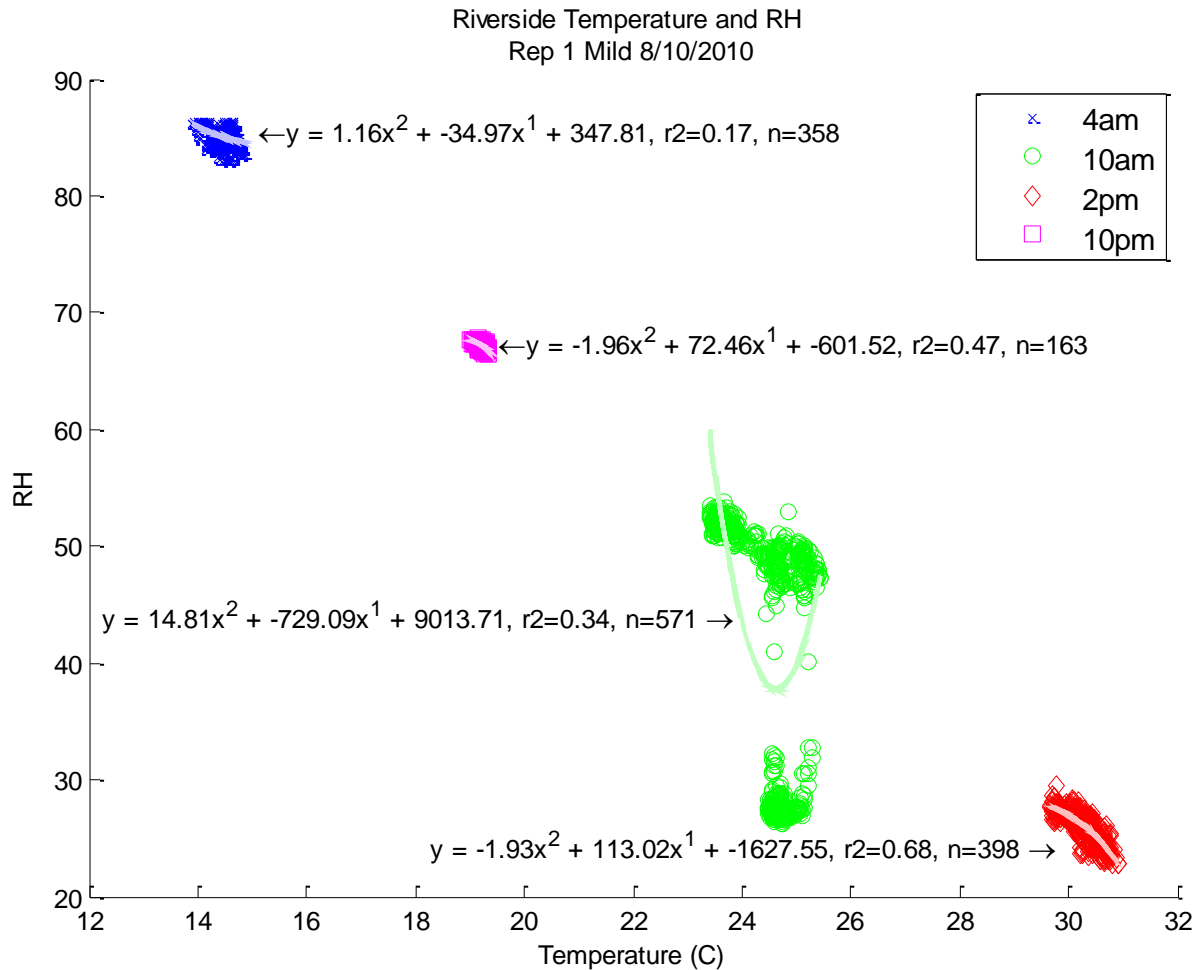
Figure 22 Regression of temperature vs. RH over Riverside for Rep 1 during mild weather

The RH over Riverside changes drastically during heat wave weather as compared to the case of mild weather. The RH drops to an extremely low value by 10am and remains through the day and does not recover in the evening. Already during the 4am run, there is a faster decrease in RH as the temperature increases. The RH during the 2pm run shows a higher RH than the 10am, though very slight. This could be because of the high amounts of evapotranspiration from the surrounding vegetation, allowing small amounts of moisture back into the air. Interestingly, the slope of the regression during 2pm run is very slight, showing little change in RH even with the continued increase in temperature. This could be the point at which the evapotranspiration rate

into the air was in equilibrium with the rate at which the air was dried by the heat. In this case, there is a relatively low correlation during each of the time periods with the greatest r^2 value being 0.55. This indicates that temperature may not be the only variable that affects RH. As discussed earlier, lack of water sources may cause RH and temperature to be less correlated. At a certain degree, as seen in the figure, although temperature is rising, there is not enough moisture in the air for the RH to fall any lower.
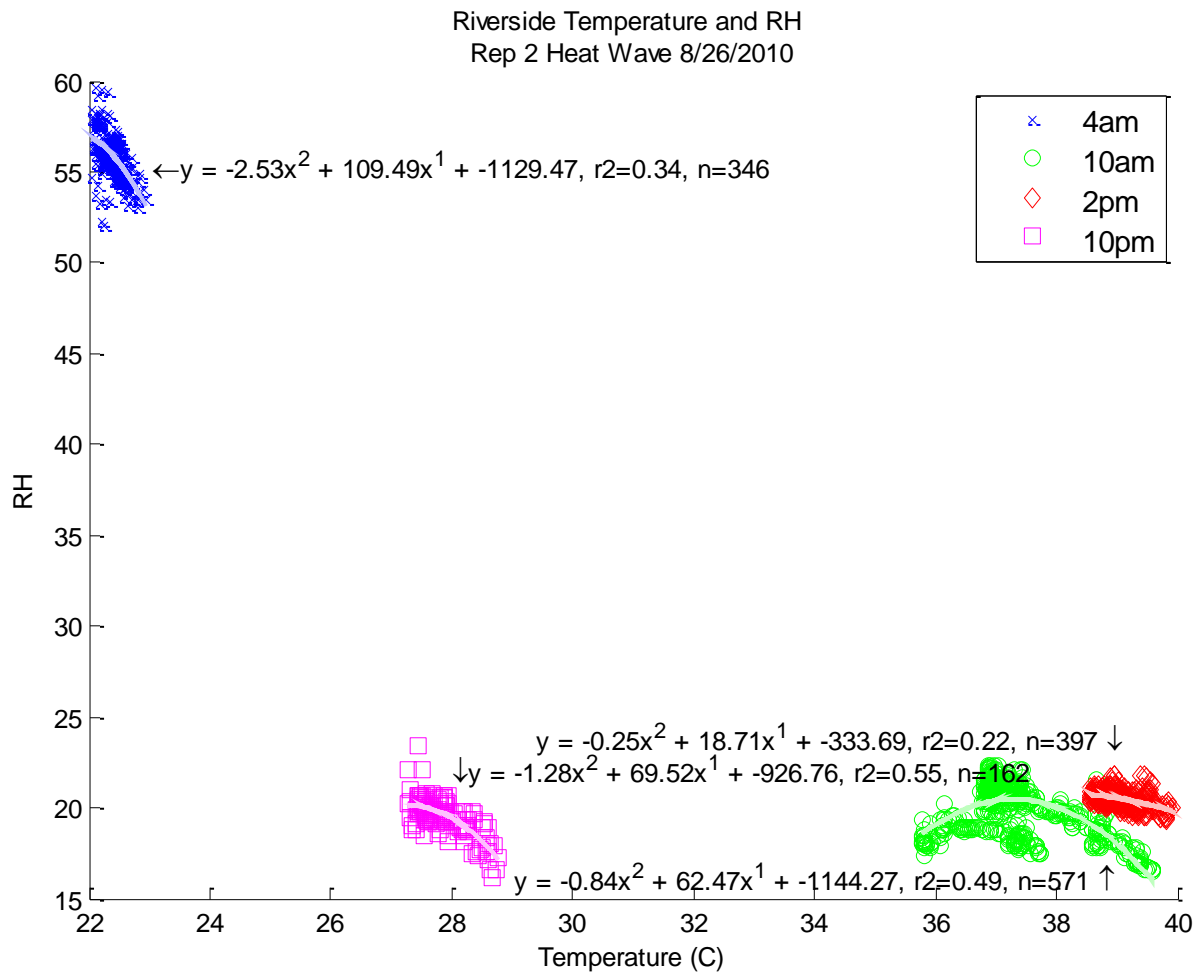
Figure 23 Regression of temperature vs. RH over Riverside for Rep 2 during a heat wave

The RH varies inversely with the temperature as shown by the negative sloping correlations. Over Pomona Rep 1, a strong correlation between RH and temperature occurs at all runs through the day. During mild weather, the variance of RH and temperature follow a relatively linear or elastic pattern, decreasing during the day and returning to a higher RH and lower temperature in the evening.
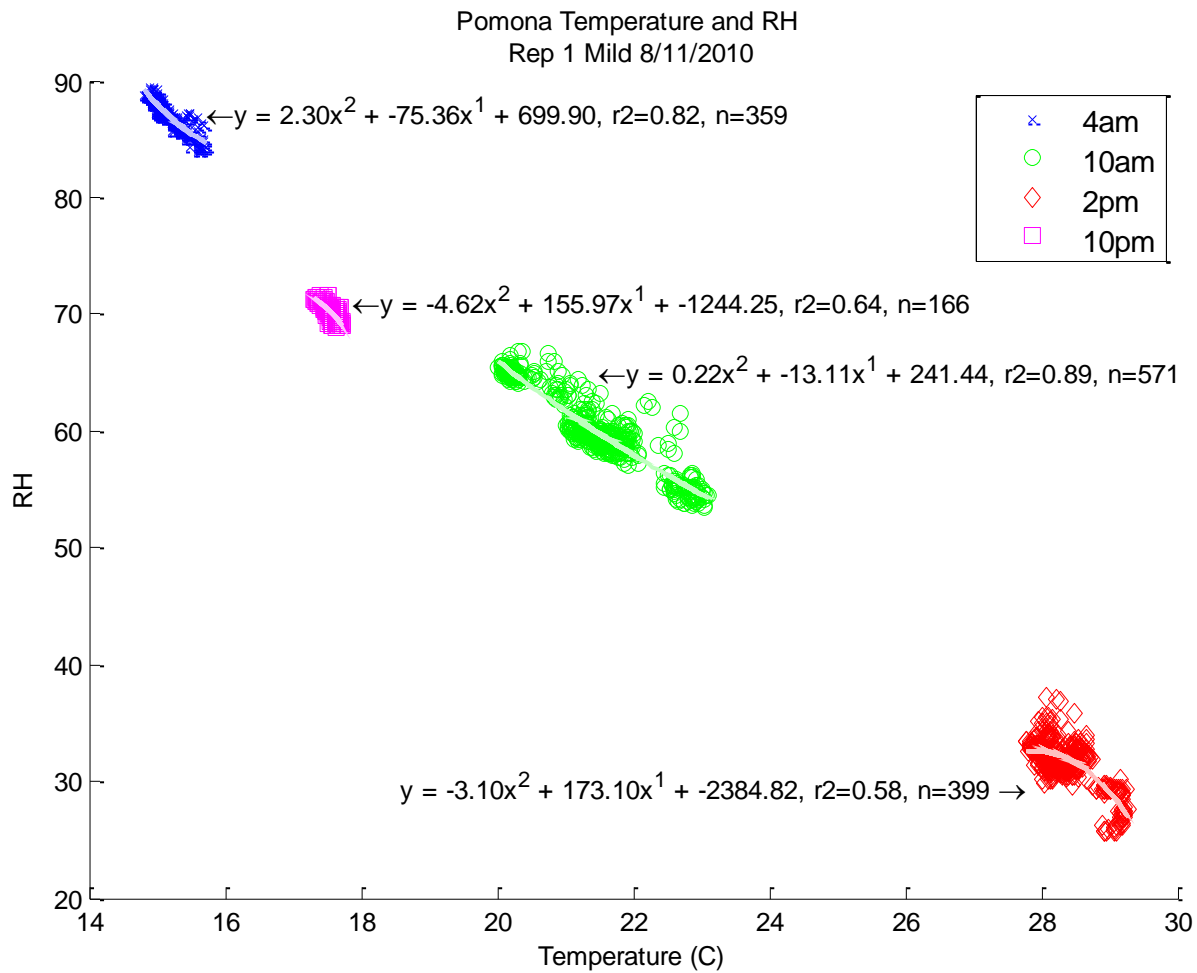
Figure 24 Regression of temperature vs. RH over Pomona for Rep 1 during mild weather

The relationship between temperature and RH is slightly different than during a day with mild weather. While mild day weather over Pomona shows a constant decrease in RH and increase in temperature that is relatively steady, during a heat wave there is a large jump between the temperature and RH during midday versus the 4am and 10pm runs. This shows a faster

recovery of RH and faster temperature drop than the mild weather. Comparing the heat wave

data over Pomona to that of Riverside there is an obvious difference between the temperature

and RH relationship and their variations through the day. Overall, the RH and temperature have

more confident correlations over Pomona than Riverside. Also, unlike Rep 2 over Riverside, the

RH over Pomona is able to recover at the end of the day and drops at a slightly slower pace,

though still faster than during mild day weather.

Figure 25 Regression of temperature vs. RH over Pomona for Rep 2 during a heat wave
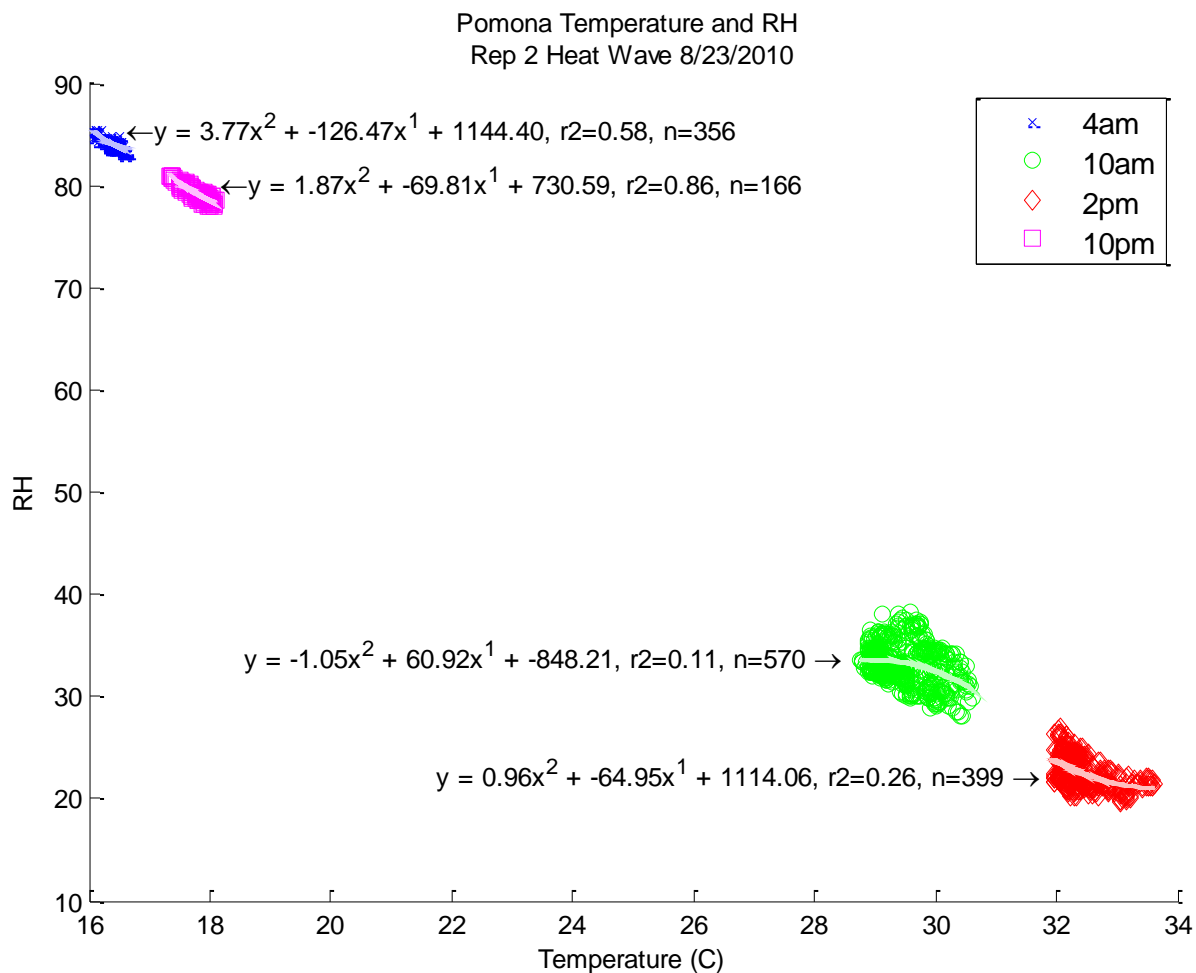
The RH varies inversely with the temperature as shown by the negative sloping

correlations. Over Mid-Wilshire, a strong correlation between RH and temperature occurs at all

runs through the day. During mild weather, the variance of RH and temperature follow a relatively linear or elastic pattern, decreasing during the day and returning to a higher RH and lower temperature in the evening. The temperature and RH during the 10am and 2pm run are relatively similar, overlapping over a large section. This indicates a more gradual increase in temperature midday. Overall, the highest temperatures over Mid-Wilshire are considerably lower than those over Pomona and Riverside. Compared to the trends seen over Riverside and Pomona, the correlation between RH and temperature is much stronger.
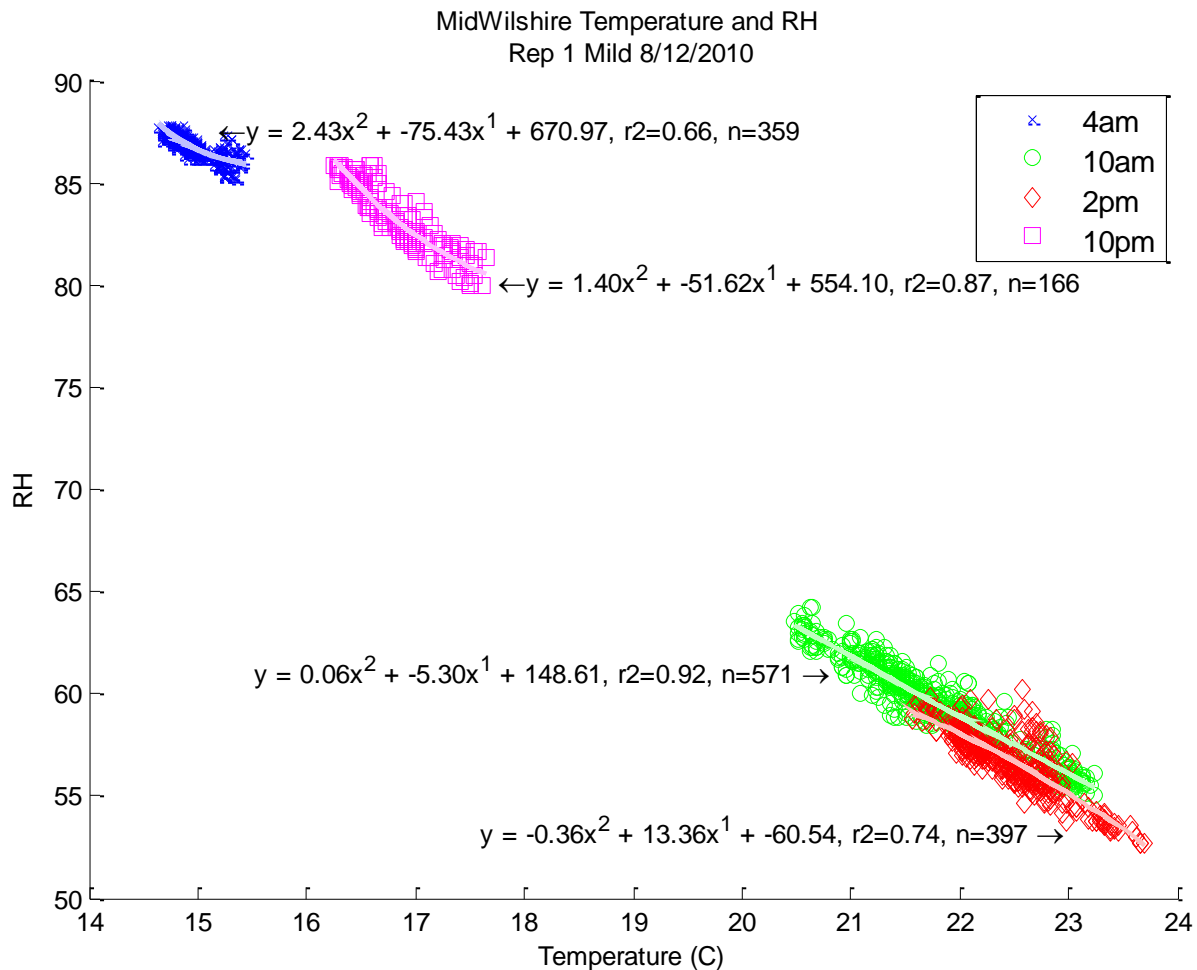
Figure 26 Regression of temperature vs. RH over Mid-Wilshire for Rep 1 during mild weather

The relationship between temperature and RH is similar to the trends seen with mild weather, but more exaggerated. The correlation confidence between the RH and temperature are lower than during mild weather. Once again, there is overlap between the 10am and 2pm run, however, the number of points which overlap is lessened as the 2pm run reaches higher temperatures. The slopes of the two runs are also drastically different. Similar to the case of Rep 2 over Riverside, the 2pm run over Mid-Wilshire has a shallow slope.

Figure 27 Regression of temperature vs. RH over Mid-Wilshire for Rep 2 during a heat wave
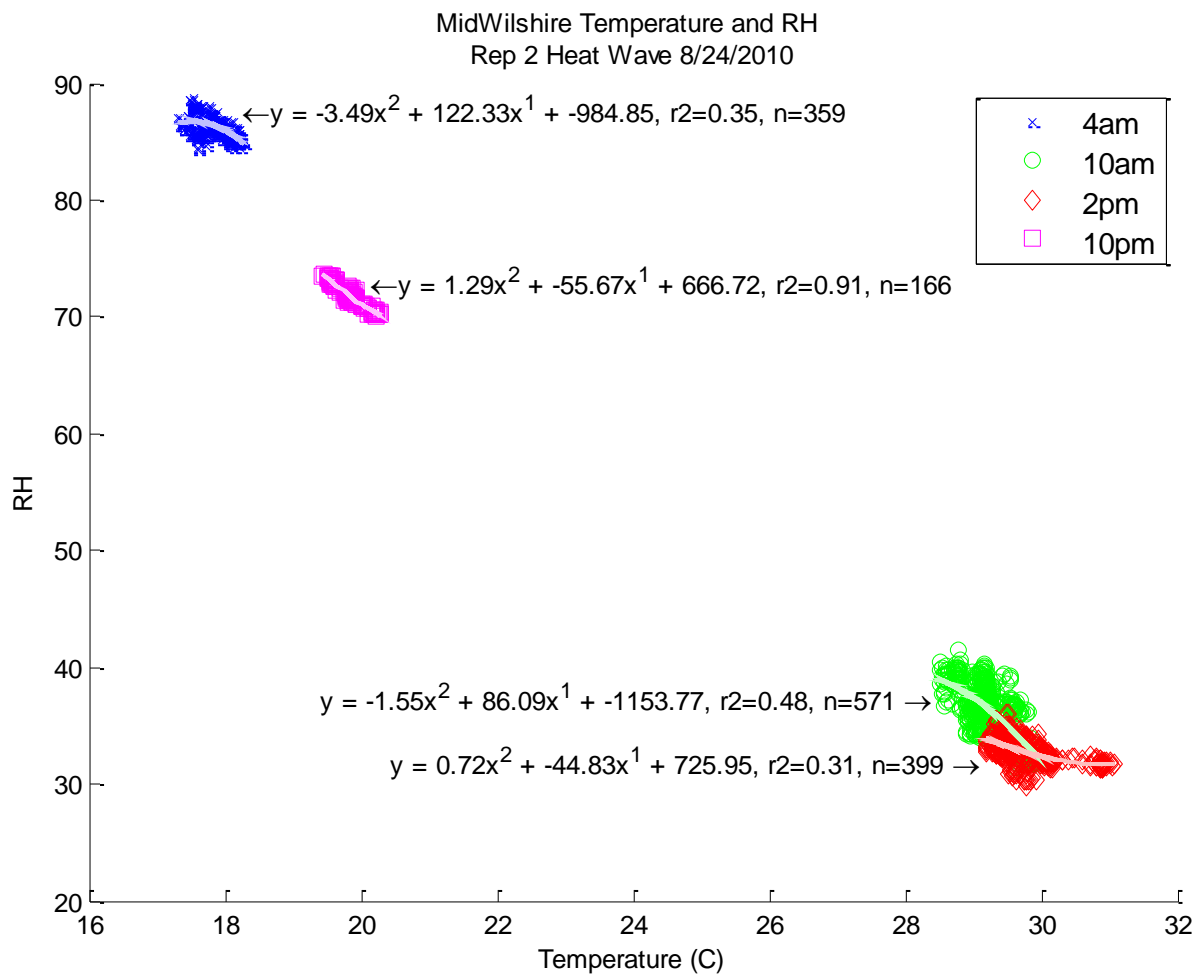
The RH varies inversely with the temperature as shown by the negative sloping correlations. Over Venice Rep 1, a strong correlation between RH and temperature occurs at all runs through the day. During mild weather, the variance of RH and temperature follow a relatively linear or elastic pattern, decreasing during the day and returning to a higher RH and lower temperature in the evening. Unlike the other locations, there is overlap of the data points during the transitions between the different runs. This shows a comparatively gradual decrease in RH and increase in temperature throughout the day. In general, there is less variability in the RH and temperature. Compared to the trends seen over all the other locations, the correlation between RH and temperature is much stronger during mild weather with r^2 values over 0.70 for every run. The constrained variation and strong correlation between RH and temperature over Venice are most likely due to the influence of the coast. The nearby ocean mediates the temperature throughout the day and adds to the moisture in the air, keeping RH values relatively high even in midday.
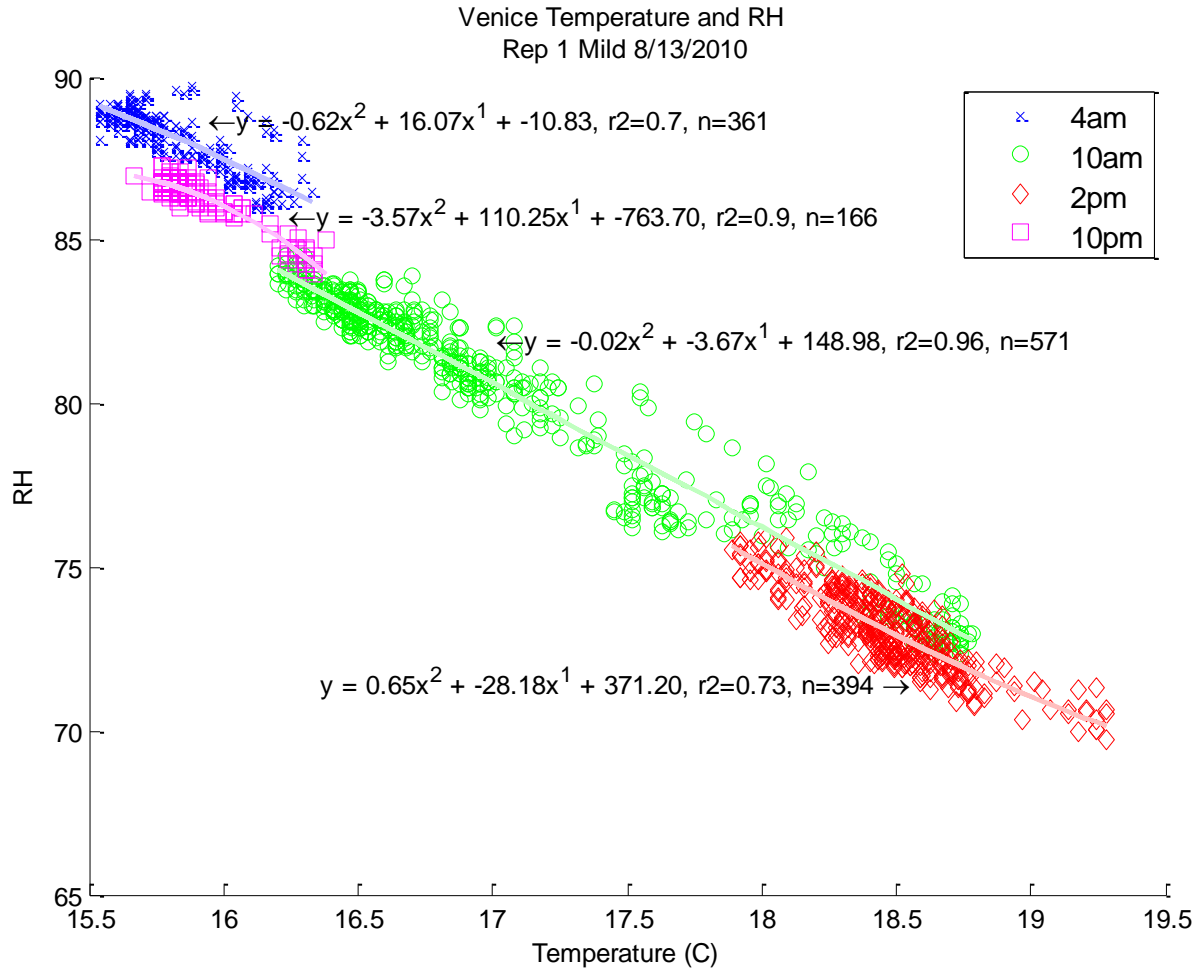
Figure 28 Regression of temperature vs. RH over Venice for Rep 1 during mild weather

The relationship between temperature and RH during a heat wave over Venice is

dramatically different than any other repetitions over the other locations. The difference between

the midday runs and the 4am and 10pm runs is similar to the previous locations with a separation

between the two pairs. However, the RH and temperature levels are switched between the pairs.

Unlike the other cases, the 10pm run has the lowest temperature and highest RH. The 10am run

experiences the highest temperatures and lowest RH. Typically, 2pm is the hottest, driest run

while 4am is the coldest, most moist run. This is most likely due to the available water source.

Because the ocean is readily available, once the temperature reaches a certain point,

evapotranspiration rates will increase and allow moisture to return to the air much earlier than in previous cases. The heat allows the air to become moister by 10pm than it had originally been in the morning. Once again, the correlation confidence between the RH and temperature are high over every run.
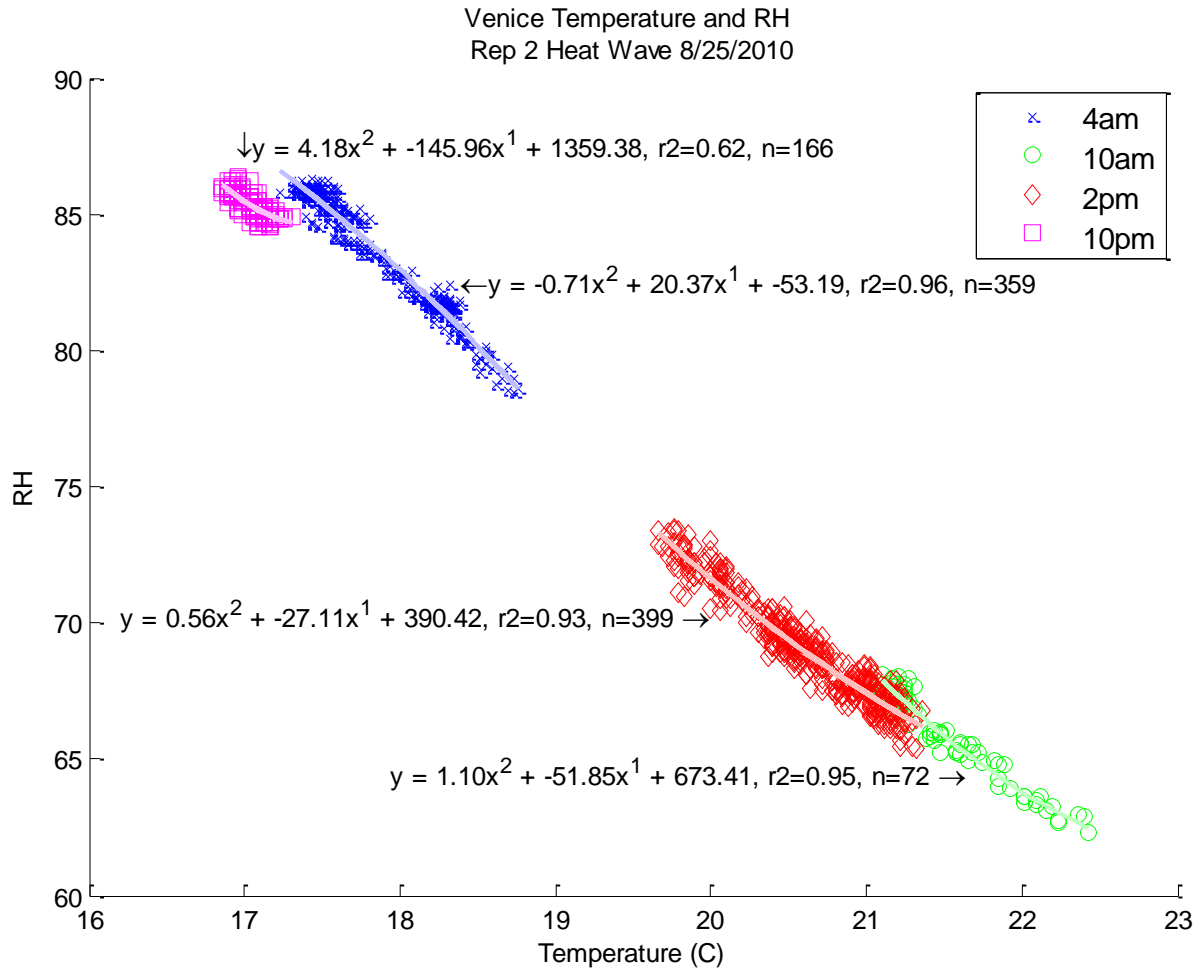
Figure 29 Regression of temperature vs. RH over Venice for Rep 2 during a heat wave
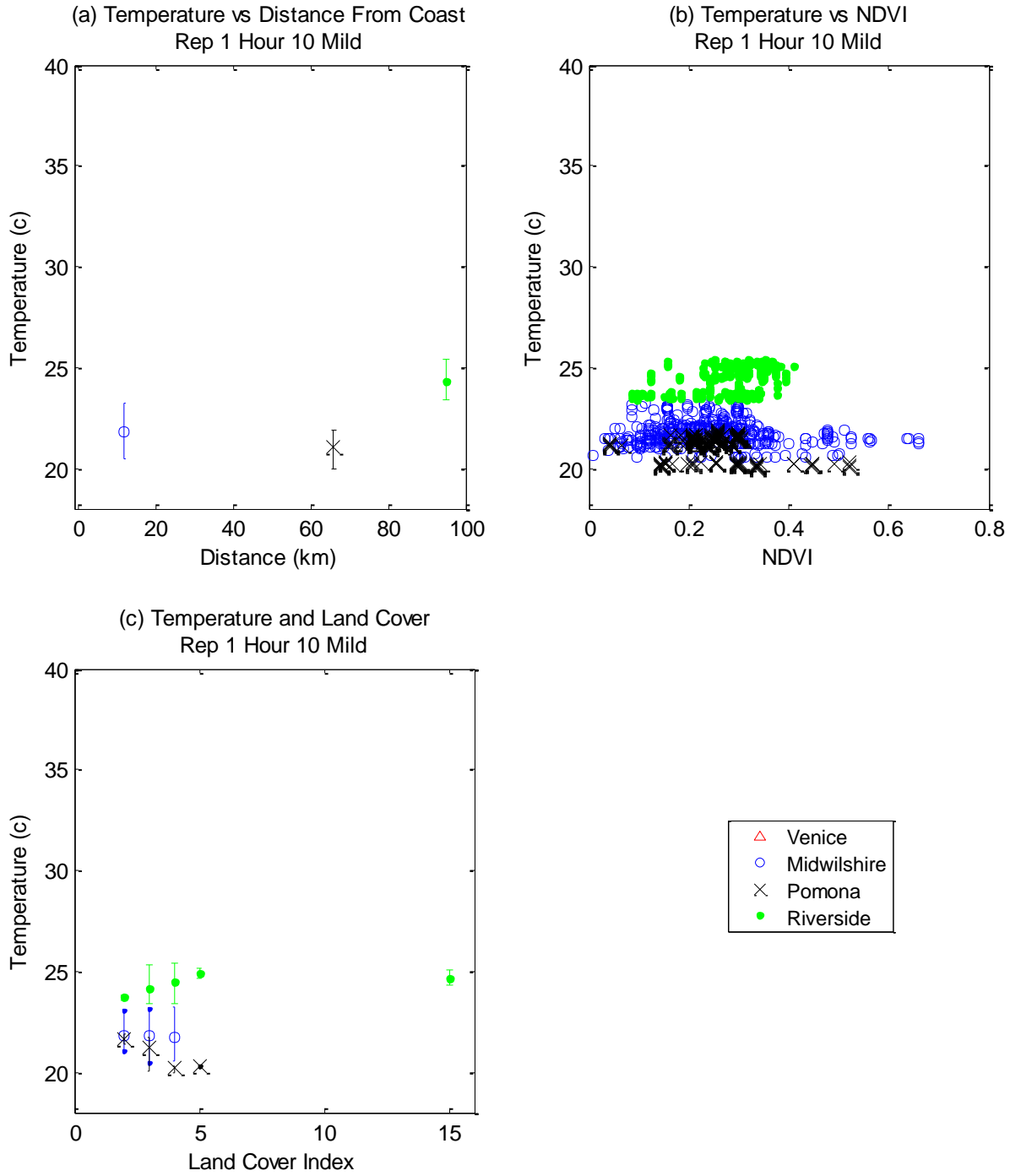
Figure 30 Temperature Comparisons with Distance from Coast, NDVI, and Land Cover for Rep 1 Hour 10. (a) and (c) display mean measured temperatures with the minimum and maximum range.
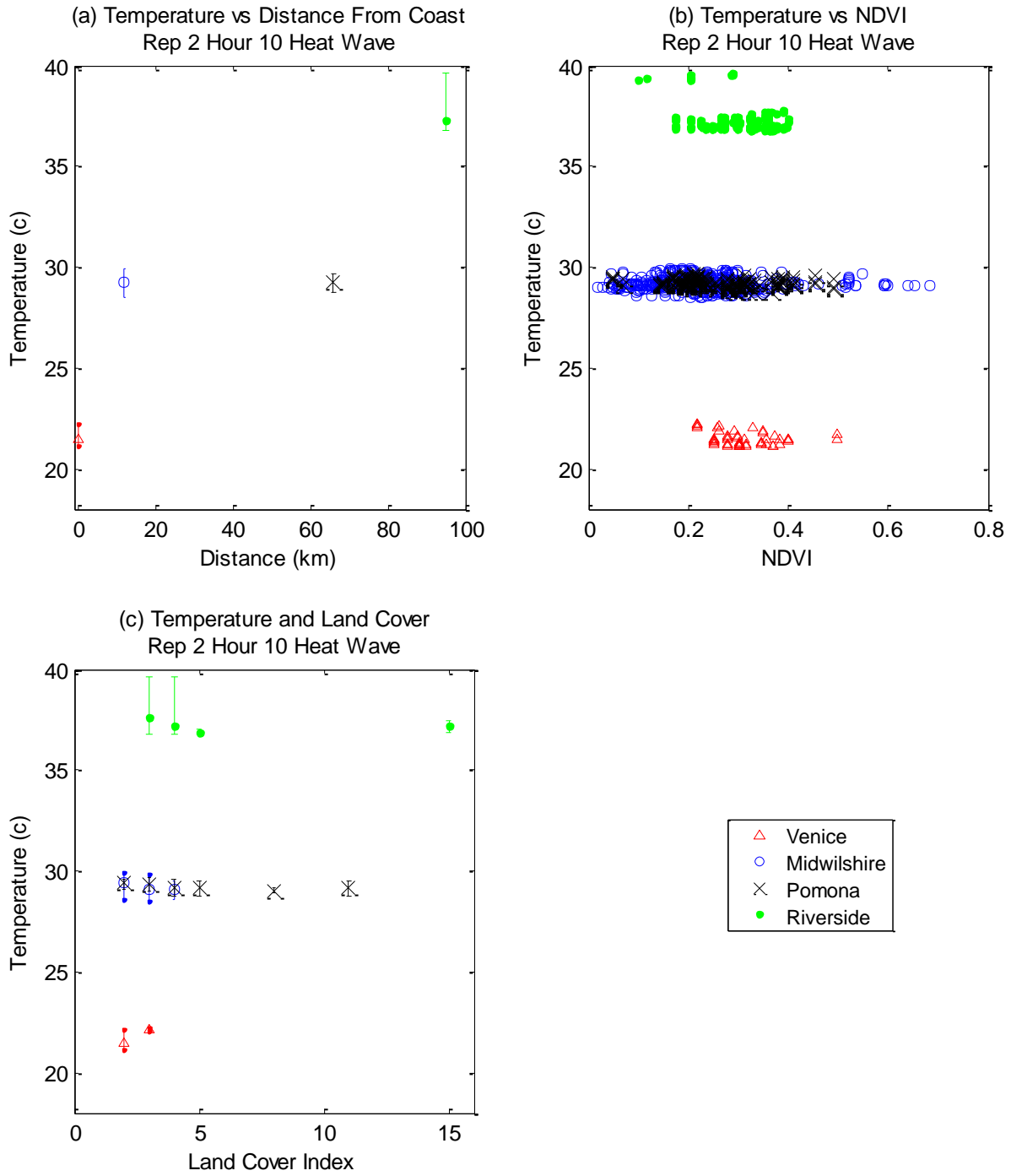
Figure 31 Temperature Comparisons with Distance from Coast, NDVI, and Land Cover for Rep 2 Hour 10. (a) and (c) display mean measured temperatures with the minimum and maximum range.
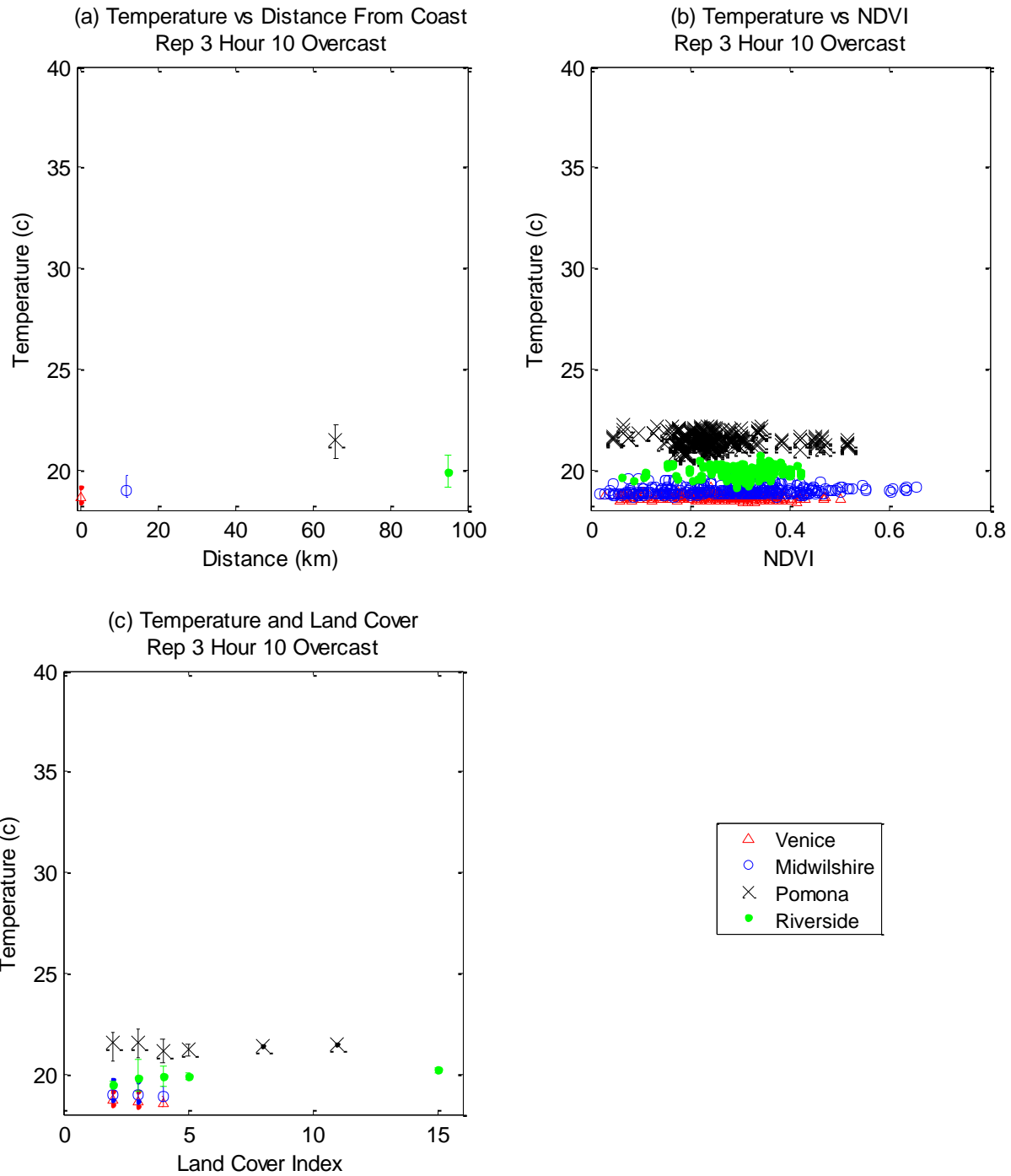
Figure 32 Temperature Comparisons with Distance from Coast, NDVI, and Land Cover for Rep 3 Hour 10. (a) and (c) display mean measured temperatures with the minimum and maximum range.
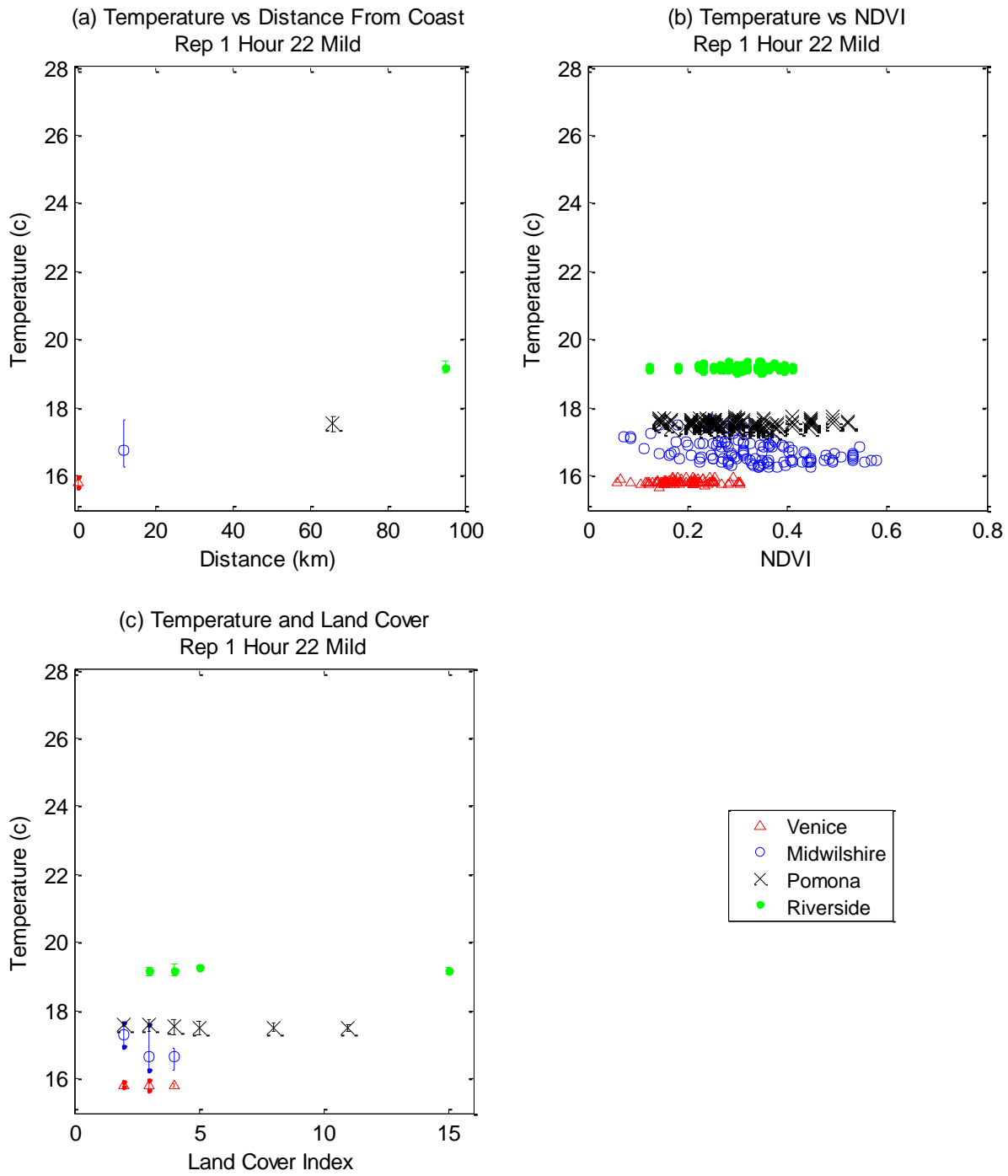
Figure 33 Temperature Comparisons with Distance from Coast, NDVI, and Land Cover for Rep 1 Hour 22. (a) and (c) display mean measured temperatures with the minimum and maximum range.
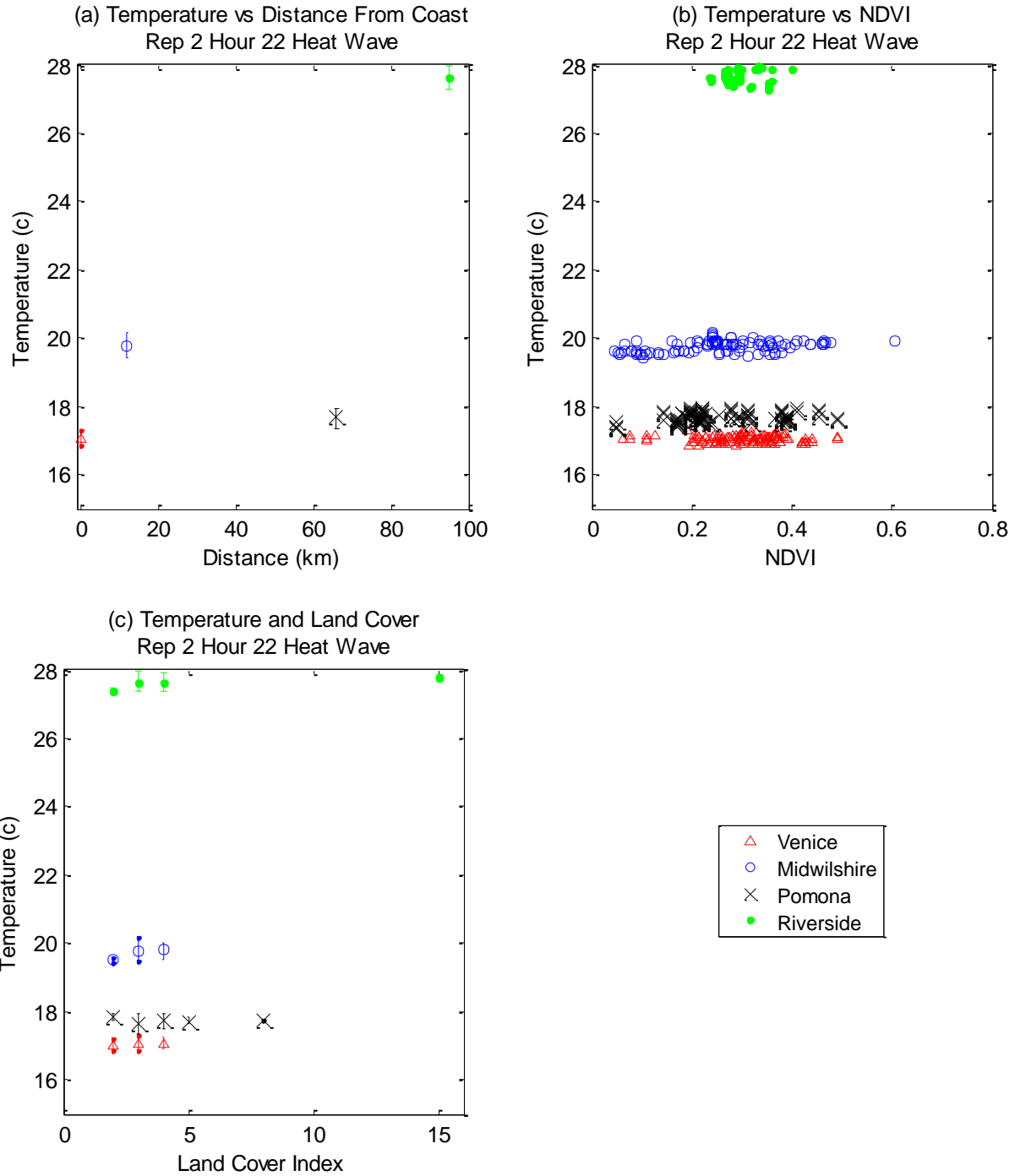
Figure 34 Temperature Comparisons with Distance from Coast, NDVI, and Land Cover for Rep 2 Hour 22. (a) and (c) display mean measured temperatures with the minimum and maximum range.
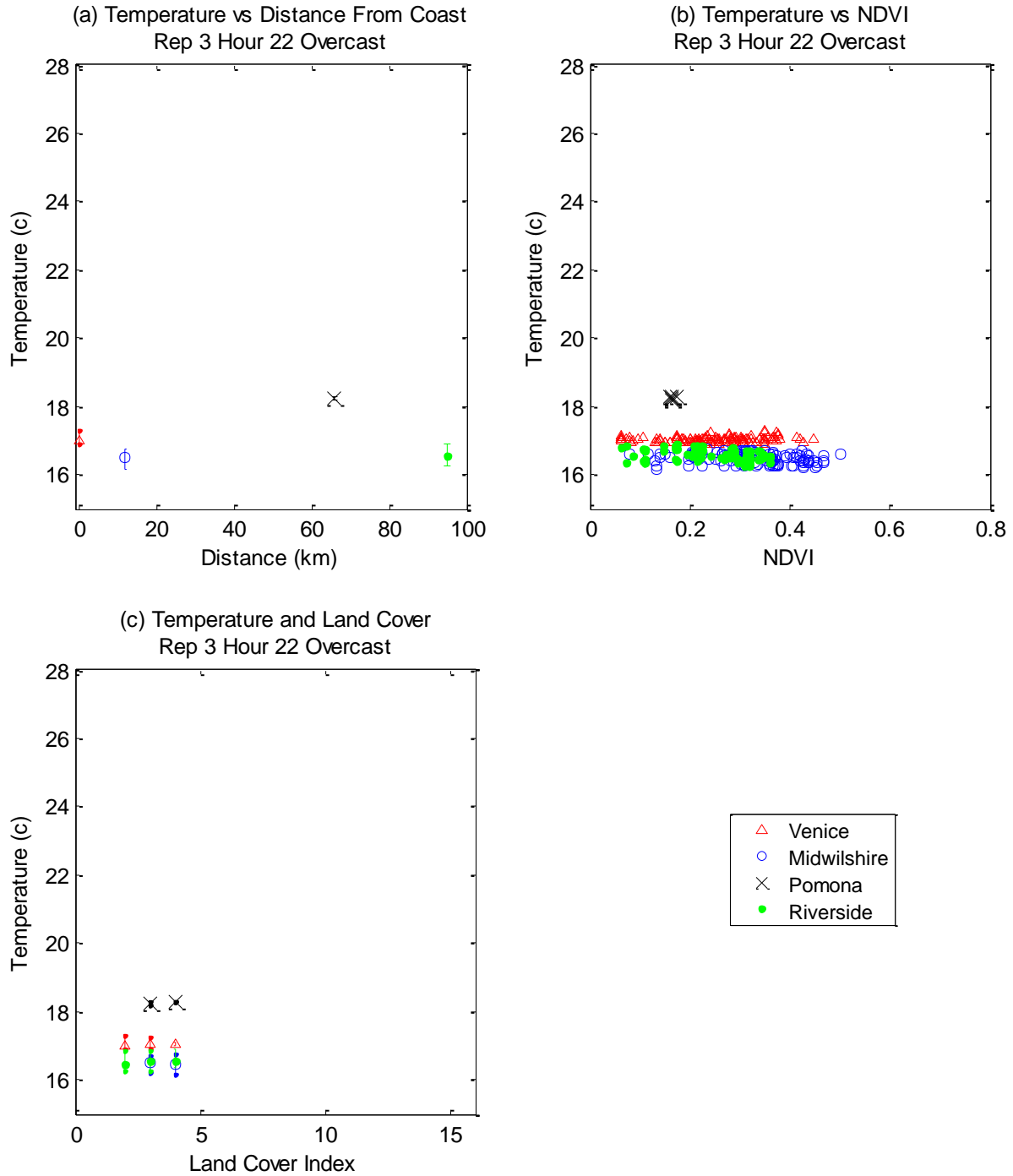
Figure 35 Temperature Comparisons with Distance from Coast, NDVI, and Land Cover for Rep 3 Hour 22. (a) and (c) display mean measured temperatures with the minimum and maximum range.

Appendix E: Matlab Code

```
%%%%%%%%%%%%%%%%%%%%%%%%%%%%%%%%%%%%%%%%%%%%%%%%%%%%%%%%%%%%%%%%%%%%%%%
%% UHI: Separate data into the 4 runs
%% September 18, 2012
%% Audrey Lee
%%%%%%%%%%%%%%%%%%%%%%%%%%%%%%%%%%%%%%%%%%%%%%%%%%%%%%%%%%%%%%%%%%%%%%%
clear all; close all; clc;

location = {'Venice','MidWilshire','Pomona','Riverside'};
time = [4,10,14,22];

% Separate data by hours - 4am, 10am, 2pm, 10pm
Llimit4 = 7/24; % To 7am (4)
Llimit10 = 12.05/24; % To 12pm (10)
Llimit14 = 18/24; % To 6pm (14)
Llimit22 = 23.99/24; % To Midnight (22)

for rep = 1:3
    for loc = 1:4

        % Load data
        % Cut GPS data
        data = load(['E:\UrbanHeatIslands\GISmaps\',location{loc},'\',...
        location{loc},'_GPS_rep',num2str(rep),'.txt']);
        hr = 3;
        % Cut station data
%        data = load(['E:\UrbanHeatIslands\Data\',location{loc},...
%            'sta_rep',num2str(rep),'.txt']);
%        hr = 1;
        % Cut normal data
%        data = load(['E:\UrbanHeatIslands\Data\',...
%            location{loc},'_rep',num2str(rep),'.txt']);
%        hr = 1;

        % Separate by hour
        DOY = fix(data(:,hr));
        hour = data(:,hr) - DOY;

        limit4 = data(hour <= Llimit4,:);
            data = data(hour > Llimit4,:);
            hour = hour(hour > Llimit4,:);
        limit10 = data(hour <= Llimit10,:);
            data = data(Llimit10 < hour,:);
            hour = hour(Llimit10 < hour,:);
        limit14 = data(hour <= Llimit14,:);
        limit22 = data(Llimit14 < hour,:);

% Saved in Data folder

%        fileID4 =
fopen(['E:\UrbanHeatIslands\Data\',location{loc},'_rep',...
%            num2str(rep),'_4.txt'],'w');
%        fileID10 =
fopen(['E:\UrbanHeatIslands\Data\',location{loc},'_rep',...
```

```matlab
%            num2str(rep),'_10.txt'],'w');
%        fileID14 =
fopen(['E:\UrbanHeatIslands\Data\',location{loc},'_rep',...
%            num2str(rep),'_14.txt'],'w');
%        fileID22 =
fopen(['E:\UrbanHeatIslands\Data\',location{loc},'_rep',...
%            num2str(rep),'_22.txt'],'w');
%
%        fprintf(fileID4, '%.7f %.2f %.2f\r\n',limit4');
%        fprintf(fileID10, '%.7f %.2f %.2f\r\n',limit10');
%        fprintf(fileID14, '%.7f %.2f %.2f\r\n',limit14');
%        fprintf(fileID22, '%.7f %.2f %.2f\r\n',limit22');

fclose('all');
    end
end

%%%%%%%%%%%%%%%%%%%%%%%%%%%%%%%%%%%%%%%%%%%%%%%%%%%%%%%%%%%%%%%%%%%%%%%%%%%
%% UHI: Minimum data extents - trimming data down to the minimum extents
%% September 18, 2012
%% Audrey Lee
%%%%%%%%%%%%%%%%%%%%%%%%%%%%%%%%%%%%%%%%%%%%%%%%%%%%%%%%%%%%%%%%%%%%%%%%%%%
clear all; close all; clc;

% Find maximum and minimum of each section
% Compares for each repetition and location then by each time
% Venice Rep 2 not considered because of time constraint it causes

% Load data
location = {'Venice','MidWilshire','Pomona','Riverside'};
time = [4 10 14 22];


for t = 1:4

for step = 1:2
for rep = 1:3
    for loc = 1:4

        % Load data
        data = load(['E:\UrbanHeatIslands\Data\',location{loc},'_rep',...
            num2str(rep),'_',num2str(time(t)),'.txt']);

        DOY = fix(data(:,1));
        hour = data(:,1) - DOY;

    switch step
        case 1

        if loc == 1 && rep ==2 % Take out bad case of Venice rep 2
            continue
        end
        % Find beginning and ending times
        CurrBeginTime = min(hour);
        CurrEndTime = max(hour);
```

```matlab
    if loc == 1 && rep ==1
        beginTime = CurrBeginTime;
        endTime = CurrEndTime;
    end
    if CurrBeginTime > beginTime
        beginTime = CurrBeginTime;
    end
    if CurrEndTime < endTime
        endTime = CurrEndTime;
    end
    if loc == 4 && rep == 3
        beginTime = beginTime + 15/(60*24); % Allow for 10 min spin up
        endTime = endTime - 4/(60*24); % Allow for 4 min cool down
    end

    case 2
    % Trim the data to the begining and ending times and save

    trimTime = data(hour >= beginTime,:);
        hour1 = hour(hour >= beginTime,:);
    trimStd = trimTime(hour1 <= endTime,:);

    % Trim associated GPS data to similar time extents
    GPSdata =
load(['E:\UrbanHeatIslands\GISmaps\',location{loc},'_GPS_rep',...
        num2str(rep),'_',num2str(time(t)),'.txt']);

    GPSDOY = fix(GPSdata(:,3));
    GPShour = GPSdata(:,3) - GPSDOY;

    GPStrimTime = GPSdata(GPShour >= beginTime,:);
        GPShour1 = GPShour(GPShour >= beginTime,:);
    GPStrim = GPStrimTime(GPShour1 <= endTime,:);

    % Cut out data that is over 3 stdev
    avg = mean(trimStd(:,2:3));
    stdev = std(trimStd(:,2:3));
    cutBegin = avg - 3*stdev;
    cutEnd = avg + 3*stdev;

    trimTemp = trimStd(trimStd(:,2) >= cutBegin(1),:);
    trimRH = trimTemp(trimTemp(:,2) <= cutEnd(1),:);

    trimRH1 = trimRH(trimRH(:,3) >= cutBegin(2),:);
    trim = trimRH1(trimRH1(:,3) <= cutEnd(2),:);

    fileID = fopen(['E:\UrbanHeatIslands\Data\',location{loc},'_rep',...
        num2str(rep),'_',num2str(time(t)),'_trim.txt'],'w');

    fprintf(fileID, '%.7f %.2f %.2f\r\n',trim');

    fileID2 =
fopen(['E:\UrbanHeatIslands\GISmaps\',location{loc},'GPS_rep',...
```

```
            num2str(rep),'_',num2str(time(t)),'_trim.txt'],'w');

        fprintf(fileID2, '%.8f %.7f %.7f\r\n',GPStrim');

%          save(['E:\UrbanHeatIslands\Data\',location{loc},'_rep',...
%              num2str(rep),'_',num2str(time(t)),'_trim.txt'], 'trim', '-
ascii')

fclose('all');

        clearvars trim trim1
    end

        clearvars data
    end
end

end
end


%%%%%%%%%%%%%%%%%%%%%%%%%%%%%%%%%%%%%%%%%%%%%%%%%%%%%%%%%%%%%%%%%%%%%%%%%
%% UHI: Matching data points with known GPS coordinates based on time
%% recorded
%% September 17, 2012
%% Audrey Lee
%%%%%%%%%%%%%%%%%%%%%%%%%%%%%%%%%%%%%%%%%%%%%%%%%%%%%%%%%%%%%%%%%%%%%%%%%
clc; clear all; close all;

% Choose repetition

time = [4,10,14,22];
for t = 1:4
for rep = 1:3
for loc = 1:4

location = {'Venice','MidWilshire','Pomona','Riverside'};

output=(['E:\UrbanHeatIslands\Data\WithGPS\',location{loc},'_rep',...
    num2str(rep),'_',num2str(time(t)),'_GPS.txt']); % designate output file
location

% Load data
% data in form DOY, temp, RH
% GPS in form lat, lon, DOY

dataOrig = load(['E:\UrbanHeatIslands\Data\',location{loc},'_rep',...
    num2str(rep),'_',num2str(time(t)),'_trim.txt']);
GPS = load(['E:\UrbanHeatIslands\GISmaps\',...
    location{loc},'_GPS_rep',num2str(rep),'_',num2str(time(t)),'.txt']);

% Find matching times within 5 seconds
% Save the DOY, lat, lon, temp, and RH
```

70

```matlab
data = [];
% Within 5 second time span
for dataIndex = 1:length(dataOrig)
    % pnt is index in dataOrig and index is index in GPS
    [val,GPSindex] = min(abs(GPS(:,3)-dataOrig(dataIndex,1)));
    % Save points within 5 second time frame
    if val <= (5/86400)
        data = [data; dataOrig(dataIndex,1), GPS(GPSindex,1:2),
dataOrig(dataIndex,2:3)];
    end
end

% Find with exact times
% [DOY,GPSIndex,dataIndex] = intersect(GPS(:,3),dataOrig(:,1));
% data = [DOY GPS(GPSIndex,1:2) dataOrig(dataIndex,2:3)];

% CSV file
% fileID =
fopen(['E:\UrbanHeatIslands\Data\WithGPS\GPS_T_RH_CSVfiles\',location{loc},..
.
%     '_GPS_rep',num2str(rep),'_',num2str(time(t)),'_matchCSV.csv'],'w');

% Txt file

fileID = fopen(['E:\UrbanHeatIslands\Data\WithGPS\',location{loc},...
    '_GPS_rep',num2str(rep),'_',num2str(time(t)),'_match.txt'],'w');

fprintf(fileID,'%.7f %.8f %.7f %.2f %.2f\r\n',data');

fclose('all');


clearvars dataOrig GPS data

end
end
end


%%%%%%%%%%%%%%%%%%%%%%%%%%%%%%%%%%%%%%%%%%%%%%%%%%%%%%%%%%%%%%%%%%%%%%%%%%%%%%
%% UHI: Matching data points with known NDVI and Land Cover based on GPS
%% Locations
%% Oct. 26, 2012
%% Audrey Lee
%%%%%%%%%%%%%%%%%%%%%%%%%%%%%%%%%%%%%%%%%%%%%%%%%%%%%%%%%%%%%%%%%%%%%%%%%%%%%%
clc; clear all; close all;

% Choose repetition
location = {'Venice','MidWilshire','Pomona','Riverside'};
time = [4,10,14,22];

for type = 1 % 1 for NDVI, 2 for Landcover
for t = 1
for rep = 1
for loc = 1
```

```matlab
    if loc == 1||2
            matLoc = {'LA'};
            land = {'Landtype'};
            day = [20100809, 20100825, 20100910];
            landGeo = {'Landcover'};

            if type == 1

load('E:\UrbanHeatIslands\Data\Landsat\Landsat_Geolocation.mat');
                Lat = Landsat_Lat_deg;
                Lon = Landsat_Lon_deg;
            end
    else
            matLoc = location{loc};
            land = {'East_Landcover'};
            day = [20100818, 20100818, 20100903];
            landGeo = {'East_Landcover'};

            if type == 1

load(['E:\UrbanHeatIslands\Data\Landsat\',location{loc},'_Geolocation.mat']);
                Lat = Lat_deg;
                Lon = Lon_deg;
            end
    end

% Load data
% data in form DOY, temp, RH
% GPS in form lat, lon, DOY



switch type
    case 1 % NDVI
    load(['E:\UrbanHeatIslands\Data\Landsat\',...
        matLoc{1},'_',num2str(day(rep)),'.mat']);
    cover = NDVI;
%     cover = LST-273.15; % Do the same for LST
    fileID = fopen(['E:\UrbanHeatIslands\Data\WithNDVI\',location{loc},...
    '_rep',num2str(rep),'_',num2str(time(t)),'_NDVI.txt'],'w');

    case 2 % Land cover
    load(['E:\UrbanHeatIslands\Data\Landsat\',... % data
        land{1},'.mat']);
    load(['E:\UrbanHeatIslands\Data\Landsat\',... % Lat and Lon
        landGeo{1},'_Geolocation.mat']);
    if loc == 1||2
        cover = Landtype;
    else
        cover = Landcover;
    end

    fileID =
fopen(['E:\UrbanHeatIslands\Data\WithLandCover\',location{loc},...
```

72

```matlab
        '_rep',num2str(rep),'_',num2str(time(t)),'_LC.txt'],'w');
end


% Find closest Lat and Lon point
% Save as DOY, Lat, Lon, Temp, RH, NDVI/Landcover, LST
dataOrig = ...
load(['E:\UrbanHeatIslands\Data\WithGPS\',location{loc},'_GPS_rep',...
    num2str(rep),'_',num2str(time(t)),'_match.txt']);
data = [];
for dataIndex = 1:length(dataOrig)

    [latVal,latIndex] = min(abs(Lat(:,1)-dataOrig(dataIndex,2)));
    [lonVal,lonIndex] = min(abs(Lon(1,:)-dataOrig(dataIndex,3)));

    data = [data; dataOrig(dataIndex,:), cover(latIndex,lonIndex)];

end


if type == 1
    fprintf(fileID,'%.7f %.8f %.7f %.2f %.2f %.7f\r\n',data');
else
    fprintf(fileID,'%.7f %.8f %.7f %.2f %.2f %.0f\r\n',data');
end



fclose('all');

fprintf(['Finish ',location{loc},' rep',num2str(rep),' time ',
num2str(time(t))])
clearvars dataOrig cover data Lat Lon

end
end
end
end


%%%%%%%%%%%%%%%%%%%%%%%%%%%%%%%%%%%%%%%%%%%%%%%%%%%%%%%%%%%%%%%%%%%%%%%%%%
%% UHI: UHI: Temperature Comparisons with Distance from Coast, NDVI, and
%% Land Cover
%% Nov 1, 2012
%% Audrey Lee
%%%%%%%%%%%%%%%%%%%%%%%%%%%%%%%%%%%%%%%%%%%%%%%%%%%%%%%%%%%%%%%%%%%%%%%%%%
clc; clear all; close all;

f = 1; % Track number of figures
time = [4 10 14 22];
weather = {'Mild','Heat Wave','Overcast'};
location = {'Venice','Midwilshire','Pomona','Riverside'};
dist = [0,12,66,95]';
% dist = [dist,dist,dist,dist];
TempHighBound = 28;
TempLowBound = 15;
```

```matlab
for t = 4
for rep = 1:3

    temp = [];
    rh = [];
for loc = 1:4

% Land Cover

% Check for areas that don't have specific land cover type
    dataNDVI = load(['E:\UrbanHeatIslands\Data\WithNDVI\',...
        location{loc},'_rep',num2str(rep),'_',num2str(time(t)),'_NDVI.txt']);
%     dataLC = load(['E:\UrbanHeatIslands\Data\WithLandCover\',...
%         location{loc},'_rep',num2str(rep),'_',num2str(time(t)),'_LC.txt']);
    LC{loc} = load(['E:\UrbanHeatIslands\Data\WithLandCover\Stats\',...

location{loc},'_rep',num2str(rep),'_',num2str(time(t)),'_LCStats_Temp.txt']);

    if loc == 1
        venice(loc,rep) = mean(dataNDVI(:,4));
    else
        temp(loc,:) = [mean(dataNDVI(:,4)-venice(1,rep)),std(dataNDVI(:,4)-
venice(1,rep))];
    end
    NDVI{loc} = [dataNDVI(:,6),dataNDVI(:,4)];
    dist(loc,2:5) = [mean(dataNDVI(:,4)),min(dataNDVI(:,4)),...
        max(dataNDVI(:,4)),std(dataNDVI(:,4))];
    % Use Max and Mins for error bars
    distMin(loc,:) = dist(loc,2)-dist(loc,3);
    distMax(loc,:) = dist(loc,4)-dist(loc,2);
    LC{loc}(:,4:5) = [LC{loc}(:,4)-LC{loc}(:,3),LC{loc}(:,3)-LC{loc}(:,5)];

end

% Plot graph
% LC
figure(f)
errorbar(LC{1}(:,1),LC{1}(:,3),LC{1}(:,5),LC{1}(:,4),'^r','MarkerSize',7)
hold on
errorbar(LC{2}(:,1),LC{2}(:,3),LC{2}(:,5),LC{2}(:,4),'ob','MarkerSize',7)
errorbar(LC{3}(:,1),LC{3}(:,3),LC{3}(:,5),LC{3}(:,4),'xk','MarkerSize',12)
errorbar(LC{4}(:,1),LC{4}(:,3),LC{4}(:,5),LC{4}(:,4),'.g','MarkerSize',17)
% bar(temp(:,3:5),'grouped')
title({['(c) Temperature and Land Cover'];...
    ['Rep ',num2str(rep),' Hour ',num2str(time(t)),'
',weather{rep}]},'FontSize',15)
% set(gca,'XTickLabel',LC)
ylabel('Temperature (c)','FontSize',15)
xlabel('Land Cover Index','FontSize',15)
axis([0 16 TempLowBound TempHighBound])
% legend(location{1:4})
FAC = 1.05 ; %increase fontsize by this factor

h = findobj(gcf) ;
for i=1:numel(h),
```

```
    try
      % some graphic objects do not have fontsize properties
      cf = get(h(i),'fontsize') ; % current fontsize
      set(h(i),'fontsize',FAC * cf) ;
    catch
    end
end
f = f+1;

% NDVI
figure(f)
plot(NDVI{1}(:,1),NDVI{1}(:,2),'^r','MarkerSize',7)
hold on
plot(NDVI{2}(:,1),NDVI{2}(:,2),'ob','MarkerSize',7)
plot(NDVI{3}(:,1),NDVI{3}(:,2),'xk','MarkerSize',12)
plot(NDVI{4}(:,1),NDVI{4}(:,2),'.g','MarkerSize',17)
% bar(temp(:,3:5),'grouped')
title({['(b) Temperature vs. NDVI'];...
    ['Rep ',num2str(rep),' Hour ',num2str(time(t)),'
',weather{rep}]},'FontSize',15)
% set(gca,'XTickLabel',LC)
ylabel('Temperature (c)','FontSize',15)
xlabel('NDVI','FontSize',15)
axis([0 0.8 TempLowBound TempHighBound])
% legend(location{1:4})
FAC = 1.05 ; %increase fontsize by this factor

h = findobj(gcf) ;
for i=1:numel(h),
    try
      % some graphic objects do not have fontsize properties
      cf = get(h(i),'fontsize') ; % current fontsize
      set(h(i),'fontsize',FAC * cf) ;
    catch
    end
end
f = f+1;

% Distance
figure(f)
errorbar(dist(1,1),dist(1,2),distMin(1),distMax(1),'^r','MarkerSize',7)
hold on
errorbar(dist(2,1),dist(2,2),distMin(2),distMax(2),'ob','MarkerSize',7)
errorbar(dist(3,1),dist(3,2),distMin(3),distMax(3),'xk','MarkerSize',12)
errorbar(dist(4,1),dist(4,2),distMin(4),distMax(4),'.g','MarkerSize',17)
% bar(temp(:,3:5),'grouped')
title({['(a) Temperature vs. Distance From Coast'];...
    ['Rep ',num2str(rep),' Hour ',num2str(time(t)),'
',weather{rep}]},'FontSize',15)
% set(gca,'XTickLabel',LC)
ylabel('Temperature (c)','FontSize',15)
xlabel('Distance (km)','FontSize',15)
axis([-1 100 TempLowBound TempHighBound])
% legend(location{1:4})
FAC = 1.05 ; %increase fontsize by this factor
```

```matlab
h = findobj(gcf) ;
for i=1:numel(h),
    try
      % some graphic objects do not have fontsize properties
      cf = get(h(i),'fontsize') ; % current fontsize
      set(h(i),'fontsize',FAC * cf) ;
    catch ;
    end ;
end ;
f = f+1;


end
end
```

References

Akbari, H., Pomerantz, M., & Taha, H. (2001). COOL SURFACES AND SHADE TREES TO REDUCE ENERGY USE AND IMPROVE AIR QUALITY IN URBAN AREAS. *Elsevier Science*, *70*(3), 295–310.

Amorim, M., Neto, J., & Bureuil, V. (2009). Thermal Structure Identified in Mobile Transects and Thermal Channel from Satellite Landsat 7. *Revista de Geografia Norte Grande*, (43), 65–80.

Arnfield, a. J. (2003). Two decades of urban climate research: a review of turbulence, exchanges of energy and water, and the urban heat island. *International Journal of Climatology*, *23*(1), 1–26.

Brandsma, T., & Wolters, D. (2012). Measurement and Statistical Modeling of the Urban Heat Island of the City of Utrecht (the Netherlands). *Journal of Applied Meteorology and Climatology*, *51*(6), 1046–1060.

Hedquist, B. C. and Brazel, A. J. (2006). Urban, Residential, and Rural Climate Comparisons from Mobile Transects and Fixed Stations: Phoenix, Arizona. *Journal of the Arizona-Nevada Academy of Science*, *38*(2), 77–87.

Bakun, A., (1990) Global climate change and intensification of coastal ocean upwelling. *Science*, 247, 198-201.

Balling, R.C. and Brazel, S.W. (1987) Time and space characteristics of the Phoenix urban heat island. *J. Arizona-Nevada Academy of Science* 21, 75-81.

Brandsma, Theo, Dirk Wolters, 2012: Measurement and Statistical Modeling of the Urban Heat Island of the City of Utrecht (the Netherlands). *J. Appl. Meteor. Climatol.*, **51**, 1046–1060.

Brazel, A. J., & Johnson, D. M. (1980). Land Use Effects on Temperature and Humidity in the Salt River Valley, Arizona. *Arizona-Nevada Academy of Science*, *15*(2), 54–61.

Brazel, A. J., & Johnson, D. M. (2010). Arizona-Nevada Academy of Science Land Use Effects on Temperature and Humidity in the Salt River Valley , Arizona LAND USE EFFECTS ON TEMPERATURE AND HUMIDITY IN THE SALT RIVER VALLEY , ARIZONA. *Journal of the Arizona-Nevada Academy of Science*, *15*(2), 54–61.

Dorman, C. E., & Koračin, D. (2008). Response of the Summer Marine Layer Flow to an Extreme California Coastal Bend. *Monthly Weather Review*, *136*(8), 2894–2992.

Duckworth, F., & SandBerg, J. (1954). The Effect of Cities Upon Horizontal and Vertical Temperature Gradients. *American Meteorology Society*, (35), 198–207.

Engel-Cox, J. a., Holloman, C. H., Coutant, B. W., & Hoff, R. M. (2004). Qualitative and quantitative evaluation of MODIS satellite sensor data for regional and urban scale air quality. *Atmospheric Environment*, *38*(16), 2495–2509.

Fernández-González, A. (2007). Analysis of the thermal performance and comfort conditions produced by five different passive solar heating strategies in the United States Midwest. *Solar Energy*, *81*(5), 581–593.

Fortuniak, K. Klysik, J. Wibig. 2006. Urban-rural contrasts of meteorological parameters in Lodz. *Theoretical and Applied Climatology* 84: 91-101. PDF.

Fitch, D. T., Stow, D. a., Hope, A. S., & Rey, S. (2010). MODIS vegetation metrics as indicators of hydrological response in watersheds of California Mediterranean-type climate zones. *Remote Sensing of Environment*, *114*(11), 2513–2523.

Golden, J. S. (2004). The Built Environment Induced Urban Heat Island Effect in Rapidly Urbanizing Arid Regions – A Sustainable Urban Engineering Complexity. *Environmental Sciences*, *00*(0).

Grimmond, C. S. ., & Oke, T. R. (1999). Heat Storage in Urban Areas : Local-Scale Observations and Evaluation of a Simple Model. *Journal of Applied Meteorology*, *38*, 922–940.

Grimmond, C. S. ., Souch, C., & Hubble, M. D. (1996). Influence of tree cover on summertime surface energy balance fluxes, San Gabriel Valley, Los Angeles. *Climate Research*, *6*, 45–57.

Gui, S., Liang, S., & Li, L. (2010). Evaluation of satellite-estimated surface longwave radiation using ground-based observations. *Journal of Geophysical Research*, *115*(D18).

Hartz, D. a., Prashad, L., Hedquist, B. C., Golden, J., & Brazel, a. J. (2006). Linking satellite images and hand-held infrared thermography to observed neighborhood climate conditions. *Remote Sensing of Environment*, *104*(2), 190–200.

Houet, T. and Pigeon G.. 2011. Mapping urban climate zones and quantifying climate behaviors – An application on Toulouse urban area. *Environmental Pollution* 159: 2180-2192. PDF.

Jenerette, G. D., Harlan, S. L., Brazel, A., Jones, N., Larsen, L., & Stefanov, W. L. (2006). Regional relationships between surface temperature, vegetation, and human settlement in a rapidly urbanizing ecosystem. *Landscape Ecology*, *22*(3), 353–365.

Kato, S., & Yamaguchi, Y. (2005). Analysis of urban heat-island effect using ASTER and ETM+ Data: Separation of anthropogenic heat discharge and natural heat radiation from sensible heat flux. *Remote Sensing of Environment*, *99*(1-2), 44–54.

Lebassi-Habtezion, B., González, J., & Bornstein, R. (2011). Modeled large-scale warming impacts on summer California coastal-cooling trends. *Journal of Geophysical Research*, *116*(D20), 1–11.

Lin, C., Chen, W., Chang, P. , et al. 2011. Impact of the Urban Heat Island Effect on Precipitation over a Complex Geographic Environment in Northern Taiwan. *American Meteorological Society*. PDF.

Luber, G., & McGeehin, M. (2008). Climate change and extreme heat events. *American journal of preventive medicine*, *35*(5), 429–35.

Marsalek, J., Karamouz, M., Goldenfum, J., & Chocat, B. (2006). Urban water cycle processes and interactions. *UNESCO*.

Melhuish, E., & Pedder, M. (1998). Observing an Urban Heat Island by Bicycle. *Weather*, *4*(53), 121–128.

Miller, N., Hayhoe, K., Jin, J., Auffhammer, M. (2007). Climate, Extreme Heat, and Electricity Demand in California. *Journal of Applied Meteorology and Climatology*, 47, 1834-1844.

Mirzaei, P. a., & Haghighat, F. (2010). Approaches to study Urban Heat Island – Abilities and limitations. *Building and Environment*, *45*(10), 2192–2201.

Ogawa, K. (2003). Estimation of land surface window (8–12 μm) emissivity from multi-spectral thermal infrared remote sensing — A case study in a part of Sahara Desert. *Geophysical Research Letters*, *30*(2), 12–15.

Stabler, L. B., Martin, C. A., & Brazel, A. J. (2005). Microclimates in a desert city were related to land use and vegetation index. *Urban Forestry & Urban Greening*, *3*(3-4), 137–147.

Stewart, I. D. (2000). Influence of meteorological conditions on the intensity and form of the urban heat island effect in Regina. *Canadian Association of Geographers*, *2*(3), 271–285.

Sun, C.-Y., Brazel, A. J., Chow, W. T. L., Hedquist, B. C., & Prashad, L. (2009). Desert heat island study in winter by mobile transect and remote sensing techniques. *Theoretical and Applied Climatology*, *98*(3-4), 323–335.

Suomi, J., & Käyhkö, J. (2012). The impact of environmental factors on urban temperature variability in the coastal city of Turku, SW Finland. *International Journal of Climatology*, *32*(3), 451–463.

Tan, K. C., Lim, H. S., MatJafri, M. Z., & Abdullah, K. (2009). Landsat data to evaluate urban expansion and determine land use/land cover changes in Penang Island, Malaysia. *Environmental Earth Sciences*, *60*(7), 1509–1521.

Tucker, C. J., Fung, I. Y., Kelling, C. ., & Gammon, R. H. (1986). Relationship between atmospheric CO2 variations and a satellite-derived vegetation index, *3139*.

Witiw, M. R., & LaDochy, S. (2008). Trends in fog frequencies in the Los Angeles Basin. *Atmospheric Research*, *87*(3-4), 293–300.

Wan, Z. (2008). New refinements and validation of the MODIS Land-Surface Temperature/Emissivity products. *Remote Sensing of Environment*, *112*(1), 59–74.

Vogelmann, J. E., Sohl, T. L., Campbell, P. V., & Shaw, D. M. (1998). Regional Land Cover Characterization using Landsat Thematic Mapper Data and Ancillary Data Sources. *Environmental Monitoring and Assessment*, (51), 415–425.

Voogt, J. a., & Oke, T. R. (1997). Complete Urban Surface Temperatures. *Journal of Applied Meteorology*, *36*, 1117–1132.

Voogt, J. a., & Oke, T. R. (1998). Effects of urban surface geometry on remotely-sensed surface temperature. *International Journal of Remote Sensing*, *19*(5), 895–920.

Voogt, J., & Oke, T. R. (2003). Thermal remote sensing of urban climates. *Remote Sensing of Environment*, *86*(3), 370–384.

Zhang, H., N Sato, T. Izumi, et al. (2008) Modified RAMS-Urban Canopy Model for Heat Island Simulation in Chongqing, China. *American Meteorological Society* 1397: 509-524.PDF.